Direct reactions of fast-fragment knock-out by high-energy protons

V. I. Komarov

Joint Institute for Nuclear Research, Dubna

Fiz. El. Chast. Atom. Yad., 5, 419-478 (April-June 1974)

A survey is presented of the experimental research on the direct nuclear A(p, pX) reactions, where X ≡ d, ^{3}H, ^{3}He, and ^{4}He, at proton energies ~ 0.2-1.0 GeV. The physical interpretation of the data obtained in such reactions is discussed.

INTRODUCTION

This review deals with experimental investigations and the interpretation of direct nuclear A(p, pX)B reactions, where X are the lightest nuclei d, ^{3}H, ^{3}He, and ^{4}He, quasielastically knocked out from a target nucleus A with energy on the order of hundreds of MeV. An important attribute of these reactions is that the kinematics of the fast particles (incident proton, scattered proton, knock-out light fragment) is close to the kinematics of the elastic scattering pX → pX of free particles.

Reactions of this type have recently been under intensive study and there is no doubt that the development of high-current proton accelerators will serve in the nearest future as a stimulus for rapid progress in this field of nuclear physics. The appearance of new experimental data on the knock-out of fast fragments raises as a rule a lively discussion.

What is the reason for the interest in direct fragment knock-out reactions?

A definite role is assumed by the somewhat unusual nature of these reactions: When a proton having a de Broglie wavelength much smaller than the average internucleon distance in the nucleus, collides with a nucleus, fast fragments appear in the final state and their kinetic energy exceeds by tens and hundreds of times the binding energy of the nucleons in these fragments. The quasielastic kinematics of the reaction suggests that the reaction mechanism consists of a direct interaction between the incident proton and a correlated group of nucleons in the nucleus (a cluster), and consequently these reactions are a direct manifestation of the cluster structure of nuclei. This extreme point of view is contrasted with a different opinion, whereby the fragment knock-out is regarded as a direct result of the interaction of the knock-out nucleons in the final state, and the fragment knock-out has no direct bearing on the internuclear correlations of the nucleons. A discussion of this type occurred at the Conference on High-Energy Physics and Nuclear Structure[1] in connection with an interpretation of experiments on quasielastic deuteron knock-out.

The strong influence of the final-state interaction on the course of direct nuclear reactions is presently obvious even at relatively high energies. Thus, it has been convincingly known for the reaction of nucleon emission following pion absorption by a nucleus[2] that the effects due to the correlation of the nuclear nucleons are commensurate with the effects due to the final-state interaction of the emitted nucleons. Moreover, separation of these effects requires detailed measurements of reaction characteristics such as the nucleon distribution with respect to the relative energies, with respect to the angles, etc. The problem of correct allowance for the interaction of the knock-out nucleons in the final state arises, of course, also in the case of fragment knock-out reactions. However, even the qualitative features of these reactions demonstrate that the decisive factor is the direct interaction of the incident protons with the nucleon clusters in the nucleus. The main attraction in the study of knock-out reactions is indeed the hope of obtaining direct experimental information on the cluster aspects of the nuclear structure. The purpose of this review is to trace the degree to which the investigations carried out to date have brought us closer to this target.

Before we proceed to the examination of concrete studies, let us spell out the types of investigations considered below. To this end we discuss the conditions under which the study of quasielastic knock-out is of greatest interest.

The region of incident-particle energies from several hundred to a thousand MeV is at present the most promising. At energies of tens of MeV the knock-out reactions have a clearly peripheral character, so that the structure of the internal region is completely inaccessible to study.

The energy dependence of the total cross sections of the NN interactions causes the absorption of the proton waves in the nucleus to decrease sharply with increasing energy in the region 100-200 MeV, and to become minimal at 500-700 MeV. In addition, decays of highly excited states of the target nucleus produced in other channels compete with the direct knock-out reactions on the periphery of the nucleus at low energies. The interference of these processes complicates the experimental results. Strong interaction of the reaction products in the final state can distort the angular-correlation functions to such an extent that even the qualitative features of the quasielastic kinematics of the process are completely lost. Separation of the quasielastic part of the process becomes possible only if a detailed account is taken of the interaction in the final state.[3] It is also important that the main conditions for the applicability of the impulse approximation, one of the most powerful methods for analyzing direct nuclear reactions, are not very well satisfied at low energies. An increase in the energy of the incident protons to several hundred MeV greatly expands the accessible region of measurement of the kinematic variables, a fact particularly useful for the investigation of the reaction mechanism. Intensive study of quasielastic knock-out reactions at energies much higher than 1 GeV can hardly be advantageous at the present time, since the properties of the NN-scattering amplitudes themselves have been studied in this energy region much less than in the medium-energy region (especially below the meson-production threshold), and the inelastic processes of multiple meson production and excitation of numerous resonances complicate the picture greatly. This review therefore deals with the approximate incident-

proton energy region from 200 MeV to 1 GeV.

The "elementary" act of scattering of the incident proton by a cluster can occur at angles from 0 to 180° in the proton–cluster c. m. s. In small-angle scattering, the cluster acquires a small momentum and an energy comparable with its binding energy in the nucleus. Although the differential cross section of this scattering is relatively large, these conditions are not favorable for the experiments. On the one hand, one encounters here the same complications as at low incident-particle energies, and on the other, the experiments cannot yield in principle any information on the short-range correlations of the nucleons in the clusters. Measurements under conditions when the protons are scattered by the clusters through large angles, up to 180°, encounter experimental difficulties because the corresponding cross sections are small. The scattering is accompanied in this case, however, by appreciable momentum transfer to the cluster, and consequently can contain information on the nucleon correlations at small relative distances.

There is no need to prove that the investigation of these correlations is fundamental to the understanding of nuclear structure. It suffices to recall that even such a fundamental nuclear property as saturation of the nuclear density cannot be explained without introducing potentials with strong repulsion at distances $\lesssim 0.5$ F. A large variety of effective potentials with cores of various types are extensively used in different theoretical models. The direct experimental data on the behavior of nuclear nucleons at distances much smaller than the average internucleon distances are, however, exceedingly scanty. This is due primarily to the experimental difficulties of obtaining such information. The theoretical interpretation of the experiments is complicated if for no other reason than that the potential description of nucleon–nucleon systems at distances smaller than approximately 0.5 F becomes problematic owing to the fundamentally relativistic character of the interaction under such conditions. Experimental information on short-range nucleon correlations of the pairing type is particularly urgent at the present time, in connection with progress made in the microscopic approach to the study of nuclear structure. Thus, the K-harmonics method developed in the last few years[4] makes it possible to calculate the main characteristics of the lightest nuclei from the properties of real NN potentials. It has been made clear at the same time[5] that the properties of heavier nuclei with $A > 10$-20 are determined essentially by odd potentials of the type V_{33} and V_{11}. There is in fact no actual information on V_{33} and V_{11}, since the free NN distance is higly insensitive to the form of these potentials. The authors who have developed the K-harmonics method propose to obtain information on the odd potentials from an indirect method such as the study of the boundary of nuclear stability of light nuclei with large neutron excesses.

The significance of the problem stimulates research in this direction. Attempts to obtain information on the short-range nuclear correlations are made primarily in the interpretation of elastic scattering of electrons and hadrons by nuclei and of quasielastic proton knock-out reactions. The information obtained in such experiments on the nucleon correlations is indirect in character, since the actually observed quantities are single-particle densities. In this respect, reactions of quasielastic knock-out of fast fragments have the advantage that the incident particle transfers a large momentum directly to a group of nucleons, and one can consequently expect from general quantum-mechanical considerations that the process should be determined essentially by the short-range correlations in this group of nucleons.

The study of the reactions of direct knock-out of fragments under conditions of scattering at intermediate angles (for example, near 90° in the c.m.s. of the proton–cluster system) can be the source of definite spectroscopic information, such as the residual-nucleus excitation spectra, the reduced cluster emission widths, etc. However, it is clear from the foregoing that fragment knock-out accompanied by proton scattering through angles close to 180° is of interest. The present review considers therefore predominantly knock-out reactions under conditions when the momentum transferred to the fragments is large.

The first section describes the presently known experimental data, which give an idea of the experimental status of the problem. The physical interpretation of the data is discussed in the second section. The third is devoted to questions connected with the study of the "elementary" quasielastic knock-out process, namely the investigation of elastic backward scattering of protons with an energy up to 1 GeV by the lightest nuclei.

1. EXPERIMENTAL DATA

The knock-out of fast deuterons by high-energy protons was first observed in 1957 in experiments performed by L. S. Azhgirei et al.[6] with the JINR synchrocyclotron. They investigated the momentum spectra of deuterons emitted by Li, Be, C, and O at an angle 7.6° relative to a 675-MeV proton beam. The spectra were measured by magnetic analysis with a resolution $\Delta p/p$ close to 3%. The divergence angle of the beam of generated secondary particles was about 0.3°. The deuterons were separated in a beam of secondary particles with a definite ratio of the momentum to the charge (p/z) by determining the range R in an absorber installed in a scintillation-counter telescope.

The measurements have shown that the deuterons are generated under these conditions with a noticeable cross section, up to momentum values 1700 MeV/c, and an increased yield is observed in the deuteron spectra at momentum values somewhat lower than the momenta of the deuteron from elastic scattering. Elastic pd scattering was revealed in the same experiments by the difference between effects produced with D_2O and H_2O targets. The pronounced peak in the deuteron spectrum at 1626 MeV/c corresponds to recoil deuterons in elastic collisions at an angle 164° in the c. m. s. Typical secondary charged-particle spectra obtained in these experiments are shown in Fig. 1. From the kinematic similarity of the observed process with elastic pd scattering, it was concluded in ref. 6 that the deuterons are knocked out as a result of almost elastic collisions between the incident protons and quasideuteron groups within the nuclei.

It is actually impossible to indicate a two-particle process capable of increasing the deuteron yield precisely in the 1600 MeV/c region. Thus, the (p, d) neutron-pick-up reaction should produce deuterons with much higher

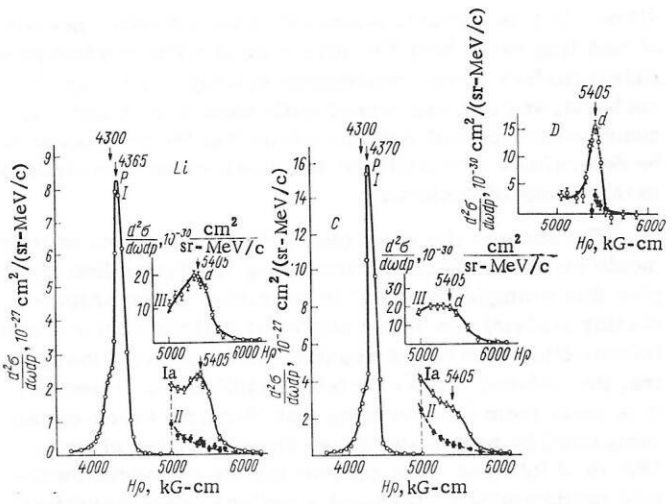

Fig. 1. Momentum spectra of secondary charged particles observed at 7.6° to a 675-MeV proton beam:[6] ○) measurement without absorber to slow down the deuteron, ●) the same with absorber; I, Ia) combined spectrum of charged particles; II) proton spectrum (the cross sections in Ia and II are magnified 100 times); III) spectrum of particles stopped in a copper absorber 18 cm thick.

momentum values – in the case of ^{12}C, without allowance for the excitation of the residual nucleus ^{11}C, the deuterons would be emitted with a momentum approximately 68 MeV/c larger than the deuteron momentum in pd scattering. The actually observed peak lies 45 MeV/c lower than the peak of the elastically scattered deuterons. Nor can the observed peaks be ascribed to possible quasifree reactions of the type

$$p + [N] \to d + \pi \tag{1}$$

or

$$p + [n] \to d + \gamma \tag{2}$$

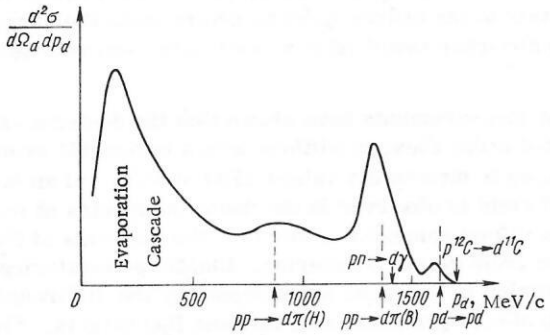

Fig. 2. Spectrum of deuterons observed at a small angle θ_d to the proton beam. For concreteness, the momenta of the deuterons from the indicated processes are given for $\theta_d = 7.6°$ and a proton energy 675 MeV; the target is ^{12}C.

on the nucleons of the nucleus (Fig. 2). Fast deuterons can be produced not only in the indicated quasi-two-particle processes, but also as a result of the development of a cascade when the incident proton passes through the nucleus. It is obvious, however, that all that can be generated in the cascade are deuterons having a rather smeared momentum spectrum without any peaks whatever, and certainly with no peaks kinematically correlated with elastic pd scattering.

The differential cross sections $(d\sigma/d\Omega)_d$ for the knock-out of deuterons, obtained in ref. 6, are given in Table 1.

The table lists the difference ΔE between the energies of the elastically scattered deuterons and the average energies of the deuterons quasielastically knocked out from the nuclei, and shows from comparison the binding energies E_b of the deuteron in the potential well of the initial nucleus. Comparison of these data indicates that the observed process can indeed be represented as the (p, pd) reaction p + (z, A) → d + p + (z – 1, A – 2), and the recoil and excitation energies of the residual nucleus (z – 1, A – 2) are relatively small – several MeV – whereas the deuterons are produced with approximate energy 600 MeV.

Attention is called to the fact that the cross sections at the observed deuteron peaks are of the same order as the cross section for elastic pd scattering under the same kinematic conditions. This correspondence confirms the conclusion that the observed deuteron knock-out is due to collisions of incident protons with quasideuteron groups:

$$p + [np] \to p + d. \tag{3}$$

It has also been indicated that a contribution can come from proton collisions with nn groups:

$$p + [nn] \to n + d, \tag{4}$$

and also with pn groups in states different from $^3S_1$ and $^3D_1$. Elastic deuteron knock-out investigated without detection of the scattered nucleon will therefore be designated as a (p, Nd) process p + (A) → d + N + (A – 2).

A more intensive study of direct knock-out reactions was initiated by a study[7] performed with the Brookhaven Cosmotron. Measurements analogous to those described above were performed at an energy (1.00 ± 0.01) GeV and in a larger volume, using targets from ^4He to Pb and detecting the deuterons at three angles θ_d, namely 5, 10, and 15°. The deuteron spectra were measured by magnetic analysis with a spectrometer (Fig. 3) having a resolution 3 MeV (width at half-height). Separation of the protons and deuterons in the spectrometer was accomplished by measuring the time of flight. Typical deuteron spectra are shown in Fig. 4. The spectra reveal distinct peaks

TABLE 1

Target nucleus	$(d\sigma/d\Omega)_d$, 10^{-27} cm²/sr	$(d\sigma/d\Omega)/z$, 10^{-27} cm²/sr	ΔE, MeV	E_b, MeV
D	0.55±0.12	0.55	—	—
Li	2.9±0.6	0.97	10	9.5
Be	2.2±0.5	0.55	23	16.7
C	3.7±0.8	0.61	30	25.2
O	4.6±1.0	0.58	33	20.7

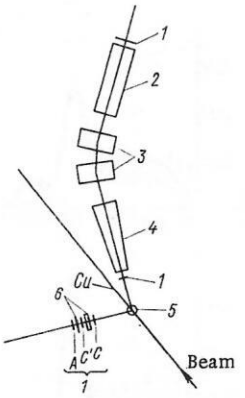

Fig. 3. Diagram of the Brookhaven setup[7] for the investigation of nuclear structure: The deuteron spectra were measured with a high-resolution spectrometer.[8] In one of the experiments, the deuterons knocked out from ^{12}C were detected in coincidence with the protons. In this case the protons were detected with a NaI counter placed in the path instead of the spectrometer; 1) counters; 2, 4) four spark chambers; 3) deflecting magnet; 5) target; 6) "R" spectrometer.

at an energy 20 MeV lower than the kinematic point for pd scattering. The sections of the spectra under the peaks were integrated to obtain the differential quasielastic knock-out cross sections.

As seen from Fig. 5a, the quasielastic knock-out angular distributions are in good agreement with the angular distributions of free pd scattering under the same kinematic conditions. The ratio of the cross sections for quasielastic knock-out to the cross sections of free pd scattering is well approximated by a power-law function $A^{1/3}$ of the mass number A of the target nucleus. Such a dependence points to a surface character to the mechanism of production of deuterons with a momentum corresponding to the quasifree kinematics: The cross section turns out to be proportional to the area of a ring of definite width Δr, with a radius r proportional to the nuclear radius.

To determine the excitation energy of the residual nucleus, using a ^{12}C target, Sutter et al.[7] measured the deuteron spectrum in coincidence with the scattered proton. The proton energy was determined from the amplitude of the pulse in a counter with a NaI scintillator. The counter was mounted at an angle ($\theta_p = 135°$) kinematically conjugate to the deuteron detection angle ($\theta_d = 8.9°$). The distribution with respect to the value of ($T_p + T_d$) of the

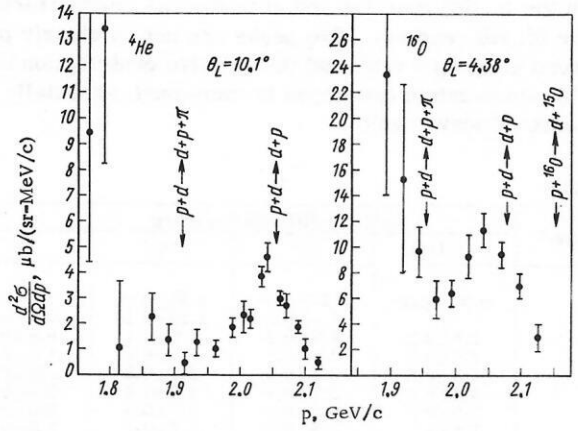

Fig. 4. Typical spectra of deuterons knocked out at a small angle θ_d to a one-GeV proton beam.[7]

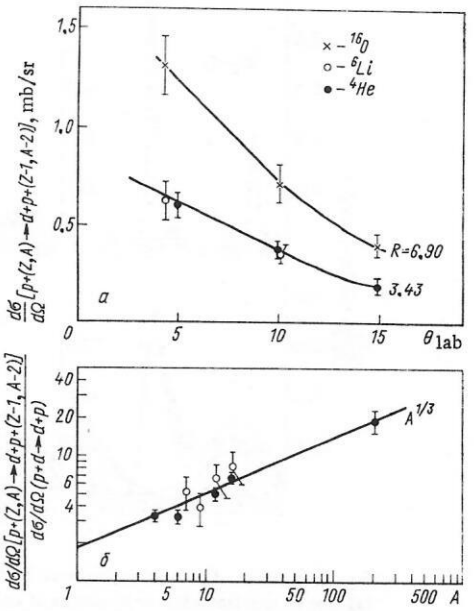

Fig. 5. Quasielastic knock-out[7] of deuterons at 1 GeV: a) Angular distributions of quasielastically knocked-out deuterons. The curves show the angular distributions of free pd scattering,[9] multiplied by a constant R. b) Dependence of the ratio of the quasielastic knock-out and free pd-scattering cross sections on the mass number A of target nucleus: ●) experimental data[7] (1000 MeV); ○) L. S. Azhgirei et al.[6] (675 MeV).

recorded events, for which the ratio of the scattered-proton energy T_p to the knocked-out deuteron energy T_d lies in the range 0.084–0.145, is shown in Fig. 6. Naturally, at a total energy resolution $\Delta (T_p + T_d) \approx 10$ MeV, separation of definite states of the residual nucleus is impossible, but it clearly follows from the obtained distribution that the reaction has the character of process (3), namely $p + {}^{12}C \rightarrow p + d + {}^{10}B$, and the ^{10}B nucleus is produced predominantly in the ground state.

A detailed investigation of the spectrum of the deuterons produced by interaction of 670-MeV protons with nuclei was undertaken by a Dubna group.[10,11] They investigated deuteron generation on nuclei in a wide of mass numbers, from Li to Pb, at four values of the deuteron-detection angle: 6.5, 9.5, 13.5, and 16° l.s. The most important factor in this study, in comparison with the experiments described above, was the larger momentum

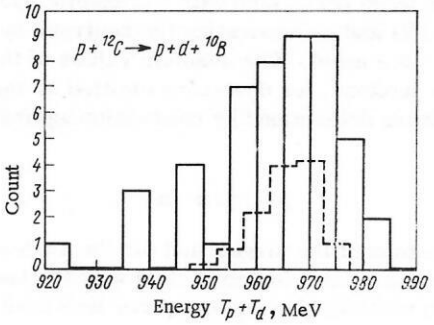

Fig. 6. Spectrum of events in the reaction $^{12}C(p, pd)^{10}B$ at an energy[7] 1 GeV as determined from the total energy $T_p + T_d$ of the fast secondary particles ($T_p/T_d = 0.084$ to 0.145): dashed line – total energy resolution of the setup, determined from free pd scattering; the curve is shifted by 27 MeV, corresponding to the deuteron binding energy in the ^{12}C nucleus.

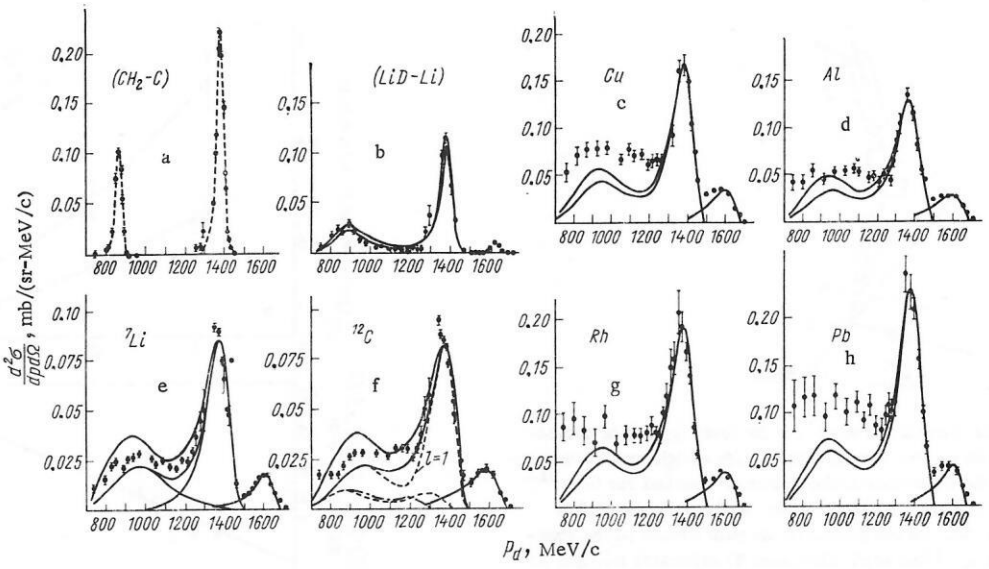

Fig. 7. Spectra of deuterons produced by 670-MeV protons at an angle $\theta_d = 6.5°$ (ref. 11): a) shape of instrumental line of spectrometer; b-h) results of calculation by the methods of dispersion theory of direct nuclear reactions; dashed curves – pole diagram; solid curves – sum of pole and triangular diagrams; dash–dot curves – interference of pole and triangular diagrams; curve with $l = 1$ show the calculation with allowance for the form factor.

interval in which the deuterons were measured. The interval from 700 to 1700 MeV/c spans under these conditions not only the kinematic region of the process (3), but also much smaller values of the momentum. It was noted already in ref. 6 that the quasielastic knock-out peaks do not stand out clearly at low deuteron energies. It was indicated that smeared deuteron peaks from the reactions

$$p + [p] \to d + \pi^+ \tag{5}$$

and

$$p + [n] \to d + \pi^0 \tag{6}$$

on the nucleon of the nucleus are possible.

The manifestation of these reactions in the deuteron spectra was assumed also in ref. 7, but only direct measurements, undertaken in refs. 10 and 11, have shown that the yield of fast deuterons with energy lower than in the quasielastic peaks can actually be attributed to reactions of meson production on intranuclear nucleons. The measurements were performed with a magnetic spectrometer ($\Delta p/p = 3.6\%$) and by separating the neutrons by time of flight ($\Delta t = 0.9$ nsec). The absolute values of the differential cross sections, for deuterons emitted at angles 6.5 and 9.5°, were determined by calibration against the reaction

$$p + p \to d + \pi^+ \tag{7}$$

on free protons of the target, and for the angles 13.5 and 16° by comparing the deuteron yield with the known yield of charged particles having an energy less than a definite threshold.

The spectra of the deuterons produced at an angle 6.5° on the nuclei ^{7}Li, ^{12}C, Al, Cu, Rh, and Pb are shown in Fig. 7. A new feature of the spectra is the intense peaks at momentum values close to the momentum of the deuteron from the reaction (7). The deuteron spectrum in this reaction (see Fig. 2) consists of two lines corresponding to deuteron emission forward in the c. m. s. ($\theta^* = 37°$, $p_d = 1378$ MeV/c) and backward ($\theta^* = 158°$, $p_d = 859$ MeV/c). The peak in the deuteron spectrum at the momentum 1360 MeV/c corresponds kinematically to deuterons emitted in the reactions (5) and (6) forward in the c. m. s. of the proton and the nucleon of the nucleus. The peak corresponding to backward emission of deuterons in the c.m.s. is much less clearly pronounced and is observed in practice only for light nuclei. The possible reason may be the broadening of the peak due to the intranuclear motion of the nucleons, the appreciable rescattering of the produced relatively slow deuterons in the residual nucleus, and superposition of other deuteron-production mechanisms, especially the cascade mechanism. The assumption that fast deuterons are produced in the meson-production processes (5) and (6) was confirmed by Monte Carlo calculations in ref. 6.

In the spectra of the deuterons at 9.5°, just as in the case $\theta_d = 6.5°$, maxima are observed in the deuteron yield from the (p, Nd) reaction and of deuterons emitted forward in the (p, πd) reaction. The peaks are not as clearly pronounced as at $\theta_d = 6.5°$, and the relative contribution of the low-momentum deuterons is increased, especially in the case of heavy nuclei.

TABLE 2

Target	dσ/dΩ at different θd, mb/sr			
	6.5° [12]	9.5°	13.5°	16°
D	0.50±0,05	0.47±0,06	0.34±0.04	—
^{6}Li	—	1.7±0,2	1.23±0.16	0.85±0.71
^{7}Li	2.1±0.2	1.9±0,2	1.0±0.1	0.8±0.1
C	2,7±0.3	2.6±0,3	1.5±0.2	1.4±0.2
Al	4.3±0.6	3.7±0,5	2.3±0.3	1.75±0.2
Cu	5.6±0.9	5.2±0,7	3.0±0.4	2.4±0.3
Rh	5.6±0.9	6.0±0,8	3.8±0.5	3.0±0.4
Pb	7.1±1.0	6.9±0,9	5.7±0.7	4.6±0.6

TABLE 3

Target	dσ/dΩ at different θ_d, mb/sr			
	6.5° [12]	9.5°	13.5°	16°
H	14.9±0.4	16.4±1.0	19.1±0.3	—
D	17.1±1.7	14.6±1.0	10.6±0.5	—
^{6}Li	—	28.5±2.0	17.0±1.4	7.7±0.5
^{7}Li	25.5±2.4	23.0±2.0	14.9±1.3	8.5±0.6
C	27.9±2.5	27±2	22.4±1.9	11.8±0.8
Al	46±4	40±3	33.1±2.7	21.6±1.5
Cu	64±6	61±5	51.8±4.3	32.7±2.3
Rh	77±7	76±6	67.0±5.6	42.5±3.0
Pb	96±7	93±7	82.2±7.0	57.6±4.0

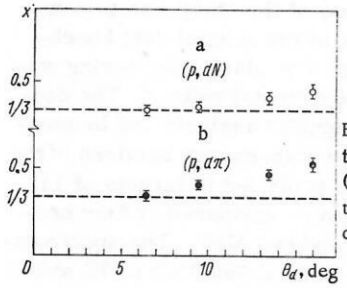

Fig. 8. Value of x when the differential cross sections of the (p, Nd) and (p, πd) reactions are approximated by the relation $d\sigma/d\Omega \sim A^x$ at different deuteron emission angles.[11]

The angle $\theta_d = 13.5°$ is the limit for the emission of deuterons in the reaction (7) on free protons at 670 MeV. The spectra measured at this angle therefore reveal in the case of light nuclei only broad maxima at an approximate momentum 1100 MeV/c, and in the case of heavy nuclei they decrease monotonically with increasing momentum. The reactions (5) and (6), just as (3) and (4), can hardly be separated at the angle $\theta_d = 16°$.

To determine the differential cross sections for the quasielastic knock-out, the high-momentum parts of the spectrum were approximated in ref. 11 by a Gaussian distribution (Table 2).

The differential cross sections for the production of a deuteron with momentum above 700 MeV/c, after subtracting the contribution of the quasielastic knock-out, are shown in Table 3. It can be assumed that in the case of light nuclei the decisive contribution to these cross sections is made by the reaction (1), and its two kinematic peaks constitute production of deuterons forward and backward in the c. m. s. In the case of nuclei heavier than carbon, the cross sections indicated in Table 3 are only partially determined by the (p, πd) reaction on these nuclei.

The errors in the cross sections listed in Tables 2 and 3 are determined not only by the statistical errors of the experiments, but also by the errors of the corrections in the spectra and by the errors of the cross sections used for the absolute normalization. Table 2 takes into account also the uncertainty due to the approximation of the high-energy sections of the spectra by a Gaussian distribution.

The dependence of the cross sections of both reactions on the mass number A of the target nucleus is well described by the power-law relation $d\sigma/d\Omega \sim A^x$. The values of x obtained in ref. 11 by least squares are shown in Fig. 8. For the knock-out process (p, Nd) the value of x is 1/3, as in ref. 7, and within an error range of approximately 10-15% it does not depend on the deuteron detection angle. For the cross sections for deuteron production in the interval 700-1500 MeV/c, the value of x is close to 1/3 at $\theta_d = 6.5°$, but increases to ~ 0.5 with an increasing detection angle, possibly because of the increased contribution made to this region of the deuteron spectrum by processes other than (p, πd).

It is typical that the angular distribution of the quasielastic knock-out cross section is similar to the angular distribution of the elastic pd-scattering cross section: Both cross sections decrease with increasing deuteron-detection angle. The cross-section ratio

$$n_{dA} = \frac{d\sigma}{d\Omega}(p, Nd) \Big/ \frac{d\sigma}{d\Omega}(pd \to pd)$$

changes by not more than 40% (Table 4). Table 4 lists also the corresponding ratios of the cross sections for the production of deuterons in the kinematic region of the (p, πd) process:

$$n_{NA} = \frac{d\sigma}{d\Omega}(p, \pi d) \Big/ \frac{d\sigma}{d\Omega}(pp \to d\pi^+).$$

A noticeable decrease of the ratios n_{NA} with increasing angle θ_d was qualitatively explained in ref. 11 as being due to the strong angular and energy dependence of the cross section of the process (7). In the case when analogous processes take place on nucleons of the nucleus, comparison with the reaction on free protons calls for averaging the cross sections with allowance for the intranuclear nucleon motion.

The emission of deuterons from the ^{12}C nucleus under the influence of 730- and 1260-MeV protons was investigated by V. S. Borisov et al.[13] Particles emitted from the target at an angle 13° to the direction of the primary beam (Fig. 9) were momentum-analyzed in a magnetic field and detected with a scintillation-counter hodoscope C_1-C_6 with

TABLE 4

Target	θ_d					
	6.5°		9.5°		13.5°	
	n_{dA}	n_{NA}	n_{dA}	n_{NA}	n_{dA}	n_{NA}
H	—	1	—	1	—	1
D	1	1.15±0.05	1	0.69±0.04	1	0.56±0.02
^{6}Li	—	—	3.62±0.14	1.74±0.07	3.62±0.15	0.80±0.04
^{7}Li	4.22±0.17	1.71±0.07	4.04±0.16	1.41±0.06	2.94±0.12	0.78±0.04
C	5.40±0.22	1.77±0.08	5.53±0.22	1.63±0.07	4.50±0.18	1.17±0.05
Al	8.60±0.38	3.09±0.13	7.87±0.32	2.43±0.10	6.76±0.27	1.73±0.07
Cu	11.07±0.48	4.27±0.19	11.06±0.44	3.70±0.15	8.82±0.35	2.71±0.11
Rh	12.07±0.48	5.11±0.22	12.77±0.51	4.63±0.19	11.18±0.44	3.51±0.14
Pb	14.01±0.54	6.45±0.27	14.68±0.59	5.67±0.23	16.76±0.67	4.30±0.17

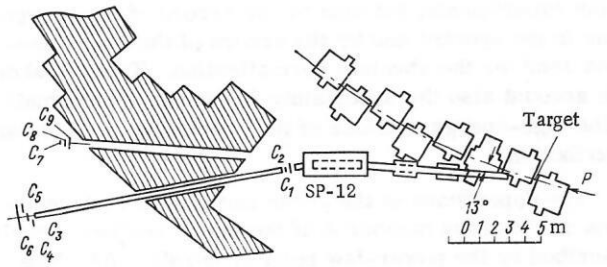

Fig. 9. Setup used in experiments on deuteron knock-out[13] at energies 730 and 1260 MeV.

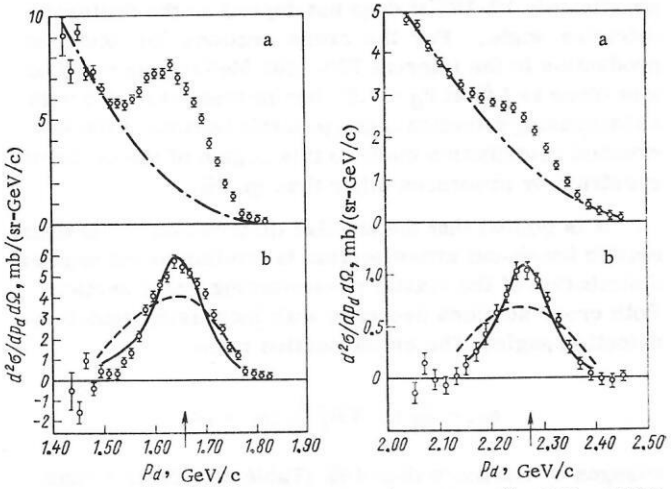

Fig. 10. Spectra of deuterons knocked out from a target[13] at 730 and 1260 MeV. a) Combined spectrum; b) quasielastic-deuteron spectrum, $\theta_d = 13°$. Dashed curve — calculation in the dispersion-theory pole approximation.

a flight base 16.6 m, for the purpose of separating the deuterons by the time of flight.

The momentum resolution of the apparatus was 4.6% at $T_p = 730$ MeV and 2.8% at $T_p = 1260$ MeV. The spectra obtained are shown in Fig. 10. The arrows show the value of the deuteron momentum from elastic pd scattering.

The spectra reveal a rather distinct peak at 730 MeV and a definite irregularity at 1260 MeV. The quasielastic knock-out differential cross section was estimated in ref. 13 by subtracting from the experimental spectra the background determined by the smooth line joining the experimental points on both sides of the quasielastic maximum. The uncertainty of this procedure makes a noticeable contribution to the error of the deuteron widths determined in this experiment (~ 15% according to the estimates of ref. 13).

The energy dependence of the quasielastic knock-out of deuterons was investigated with the JINR synchrocyclotron in ref. 14. The purpose of the study was to compare the energy dependences of the quasielastic knock-out and elastic pd scattering. The elastic scattering was measured with the same experimental setup.[15] The deuterons were separated by magnetic analysis and by measuring the time of flight. The high-energy sections of the spectra of the fast deuterons produced in targets of Li, Be, and C at a lab angle 5.5° were measured at four proton energies, 382, 484, 578, and 666 MeV. The spectrometer resolution ranged from 3.5% at 666 MeV to 7% at 382 MeV. The quasielastic knock-out peaks were clearly distinguished on the experimental curves at the energies 484, 578, and 666 MeV (Fig. 11). This has made it possible to approximate the experimental spectra by sums of two Gaussian curves, all six parameters of which were determined by least-squares fitting to the experimental points. At 382 MeV, the mean values of the momentum and the variances of the two Gaussian curves were obtained by extrapolating values obtained at higher energies. The quasielastic knock-out cross sections given in Table 5 were determined as the areas under the Gaussian curves of the quasielastic peak.[14]

Table 5 gives also the ratio of the cross sections for quasielastic knock-out $(d\sigma/d\Omega)_{(p, Nd)}$ to the cross sections of free pd scattering. A comparison with the data of ref. 7 shows that in the interval 380–1000 MeV these ratios

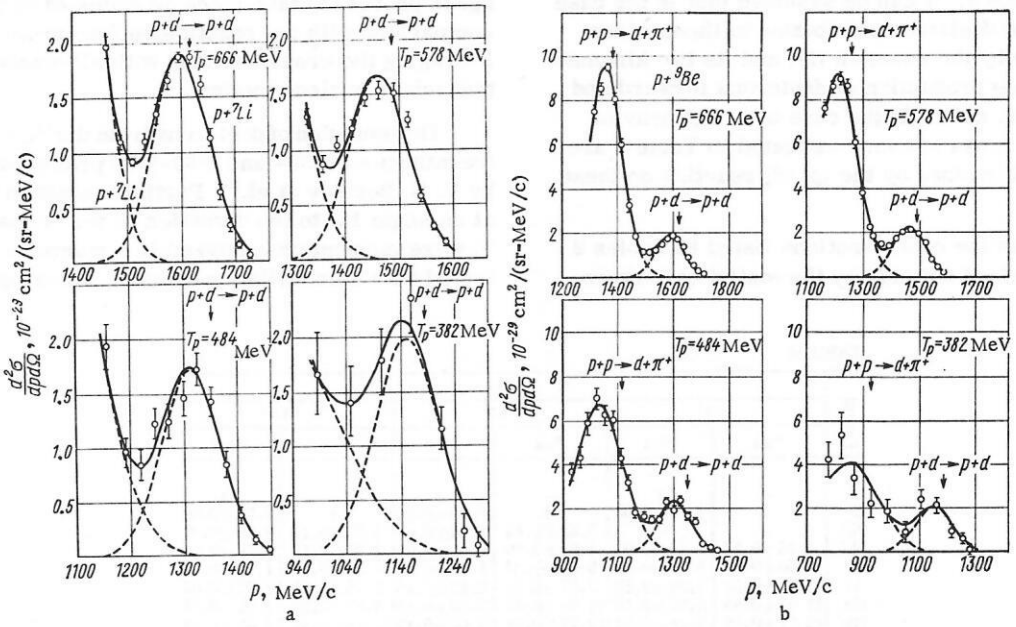

Fig. 11. Spectra of deuterons generated in the following targets: a) ^{7}Li; b) ^{9}Be at 5.5° to a proton beam of energy[14] 382, 484, 578, and 666 MeV; dashed lines — Gaussian curves obtained by least squares.

TABLE 5

Target nucleus	Energy T_p, MeV	$(d\sigma/d\Omega)(p, Nd)$, 10^{-27} cm^2/sr	$n_d = \frac{(d\sigma/d\Omega)(p, Nd)}{(d\sigma/d\Omega)_{pd}}$
^{7}Li	382	2.9±1.4	2.3±1.0
	484	2.3±1.0	2.7±0.9
	578	2.3±0.4	3.1±0.3
	666	2.4±0.35	3.7±0.2
^{9}Be	382	3.2±0.7	2.5±0.35
	484	3.3±0.8	3.8±0.5
	578	3.1±0.4	4.3±0.3
	666	2.5±0.4	3.9±0.2
^{12}C	382	5.5±1.5	4.4±0.9
	484	4.5±1.2	5.2±1.0
	578	3.9±0.5	5.5±0.4
	666	3.0±0.4	4.7±0.4

are independent of the energy of the incident protons, with an accuracy of about 20%, although the pd-scattering cross section changes by a factor 7.5 in this energy interval (see Figs. 12 and 13).

The first experiment in which knock-out of high-energy deuterons was sytematically investigated in coincidence with scattered protons was performed recently at 590 MeV by Alder et al.[16] They measured the cross section of the reaction ^{6}Li(p, pd)^{4}He in a kinematically complete experiment: The deuterons were identified by momentum and by time of flight. The proton energy was measured by range in the decelerating absorber of a scintillation-counter telescope. The direction of particle emission was detected by spark chambers. The total energy resolution was about 10 MeV. The laboratory angles of deuteron and proton detection were 43 and 58°, corresponding to scattering through 90° in the c. m. s. for free pd scattering. In this respect, the experiment differed significantly from those mentioned above, where the deuteron knock-out corresponded to proton scattering through angles close to 180° in the c.m. s. Therefore the average value of the momentum transferred to the two nuclear

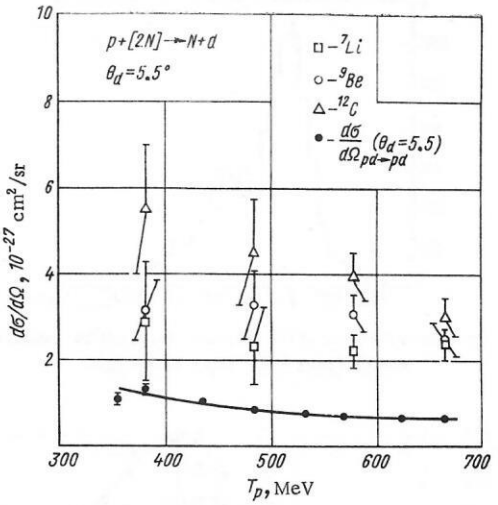

Fig. 12. Energy dependence of the differential cross section for quasielastic knock-out of deuterons from light nuclei[14] at 5.5°.

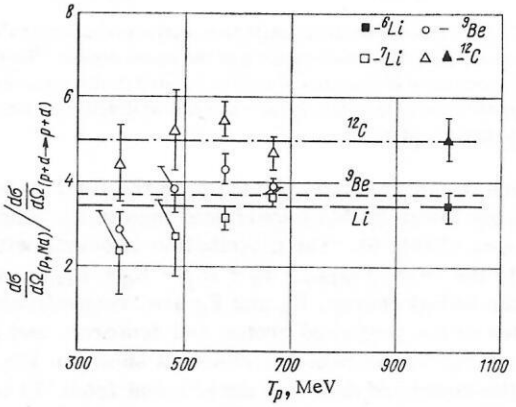

Fig. 13. Energy dependence of the ratio of the differential cross sections for quasielastic knock-out of deuterons and free pd scattering.[14,15] The experimental points at 1 GeV were taken from ref. 7.

TABLE 6

Proton energy, GeV	Detection angle, deg.		Target nuclei	Identification method	Average momentum q transferred to deuteron, F^{-1}	Reference
	deuteron	protons				
0.675	7.6	—	Li, Be, C, O	Magnetic analysis (H), range (R)	7.6	[6]
1.00 ± 0.01	5; 10; 15	—	^{4}He, ^{6}Li, ^{12}C, ^{16}O, Pb	H, time of flight (t_f)	9.3—9.1	[7]
1.00 ± 0.01	8.9	135	^{12}C	H, t_f for deuterons; pulse-height analysis in NaI counter for protons.	—	[7]
0.670	6.5; 9.5; 13.5; 16		Li, C, Al, Cu, Ru, Pb	H, t_{fd}	7.6	[10, 11]
0.73; 1.26	13	—	C	H, t_{fd}	7.8; 10.2	[13]
0.382; 0.484; 0.578; 0.666	5.5	—	^{7}Li, Be, C	H, t_{fd}	5.7—7.6	[14]
0.59	43	58	^{6}Li	H, t_f — for deuterons R — for protons	5.1	[16]
0.59	43 48	58 68	^{3}He	H, t_f — for deuterons R — for protons	5.1	[17]

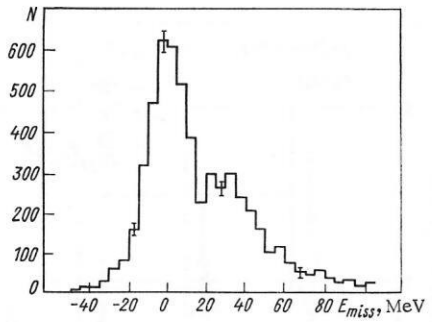

Fig. 14. Spectrum of events of the reaction ^{6}Li(p, pd)^{4}He relative[16] to the energy $E_{miss} = E_0 - (E_p + E_d + E_{rec})$.

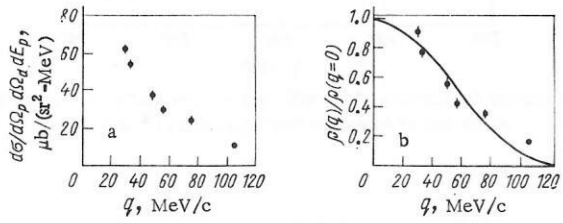

Fig. 15. Dependence of the differential cross section of the reaction ^{6}Li(p, pd)^{4}He (g·s) on the total momentum q of the recoil nucleus ^{14}He (ref. 16) (a), and momentum distribution of $\rho(q)$ calculated in the plane-wave impulse approximation (b); solid curves – theoretical distribution obtained by Yu. A. Kudeyarov et al.[43]

nucleons which produce a deuteron in the final state is noticeably lower in this experiment than in the other experiments (Table 6). The distribution of events with respect to the value $E_{miss} = E_0 - (E_p + E_d + E_{rec})$, where E_0 is the initial energy, E_p and E_d are, respectively, the energies of the scattered proton and deuteron, and E_{rec} is the energy of the recoil nucleus, is shown in Fig. 14. Since the energy of deuteron detachment from ^{6}Li is only 1.5 MeV, the principal peak near the value $E_{miss} = 0$ is interpreted as the result of quasielastic scattering of a proton by a deuteron cluster in ^{6}Li, leaving ^{4}He in the ground state. The second broader peak is probably connected with the breakup of ^{4}He. The momentum distribution of the recoil nuclei was determined from events satisfying the condition $-40 < E_{miss} < +10$ MeV. The differential cross section of the reaction as a function of the total momentum q of the recoil nucleus ^{4}He in the ground state is shown in Fig. 15.

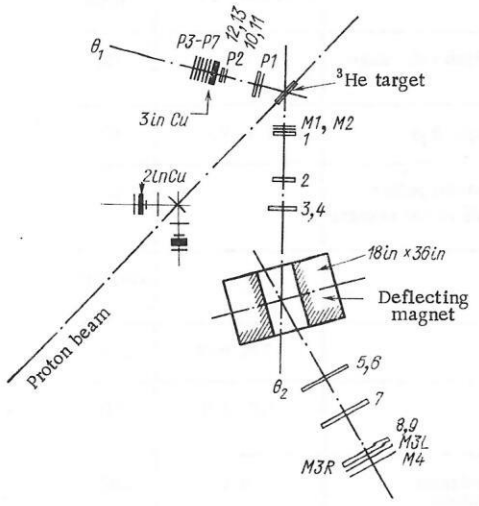

Fig. 16. Experimental setup[16,17] for investigation of (p, pd) reactions: 1-13) wire spark chambers; M1-M4 and P1-P7) scintillation counters.

The same setup (Fig. 16) was used to investigate the reaction ^{3}He(p, pd) up to a recoil-proton momentum[17] 230 MeV/c. The differential cross section of the reaction ^{3}He(p, pd)p at 590 MeV, listed in Table 7, is subject to ±15% systematic errors in addition to the indicated statistical errors.[17]

Quasielastic knock-out of clusters more complicated than the deuteron have been much less investigated. This is due primarily to the experimental difficulties, since the cross sections are small in comparison with the principal proton–nuclear interaction channels. For a reliable identification of the reaction it is necessary to separate the knock-out nuclei under conditions of high background of the extraneous and much more intense reactions. The only experiments performed at proton energies above 200 MeV prior to 1968 were experiments on the knock-out of ^{4}He from light nuclei by 660-MeV protons under conditions of small momentum transfer to the knock-out clusters.[18] The He nuclei were detected at large angles to the proton beam (70-105°). The energy of the knock-out nuclei was 10-20 MeV. The analysis of the data is therefore difficult, for the reasons discussed at the beginning of the article.

Measurements of the spectra of ^{3}He and ^{4}He nuclei knocked out from light nuclei at a small angle to the proton beam were carried out in refs. 19-21 using the JINR synchrocyclotron. The general experimental setup is illustrated in Fig. 17. The He-nuclei detection angle was 5.4° in steps of 0.1°. The processes with cross sections 10^{-30}-10^{-31} cm^2/sr were detected at a magnetic spectrometer resolution ($\Delta p/p$) close to 6%. The particles selected in effective momentum were transported by a magnetic focusing channel to a system of scintillation counters located behind the radiation shield, so as to reduce the additional counts due to scattered radiation. The nuclei ^{3}He or ^{4}He were identified in a flux of particles with definite effective momentum by selection based on time of flight, specific ionization loss, total energy release in the scintillator of the last coincidence counter, and by range.

The targets used for the study of the knock-out of ^{4}He were the nuclei ^{6}Li, ^{9}Be, and ^{12}C. The nucleus ^{6}Li has a clearly pronounced α–d structure, and one should expect the quasielastic scattering to affect most strongly the α substructure of this nucleus. The choice of ^{9}Be and ^{12}C as targets was governed by the fact that at the time the measurements were made there were available for these

TABLE 7

Detection angles	Recoil-proton momentum, MeV/c	$\frac{d\sigma}{d\Omega_p \cdot d\Omega_d \cdot dE_p}$, mb/(sr^2·MeV)	$n \cdot \rho(q)$, 10^{-7}(MeV/c)$^{-3}$
$\theta_d = 43°$ $\theta_p = 58°$	33	0.0425±0.0020	2.2±0.1
	45	0.0362±0.0016	1.87±0.08
	69	0.0226±0.0010	1.15±0.05
	96	0.0109±0.0010	0.55±0.05
$\theta_d = 48°$ $\theta_p = 68°$	134	0.0029±0.0007	0.142±0.034
	185	0.0008±0.0002	0.041±0.010
	233	0.0005±0.0001	0.022±0.005

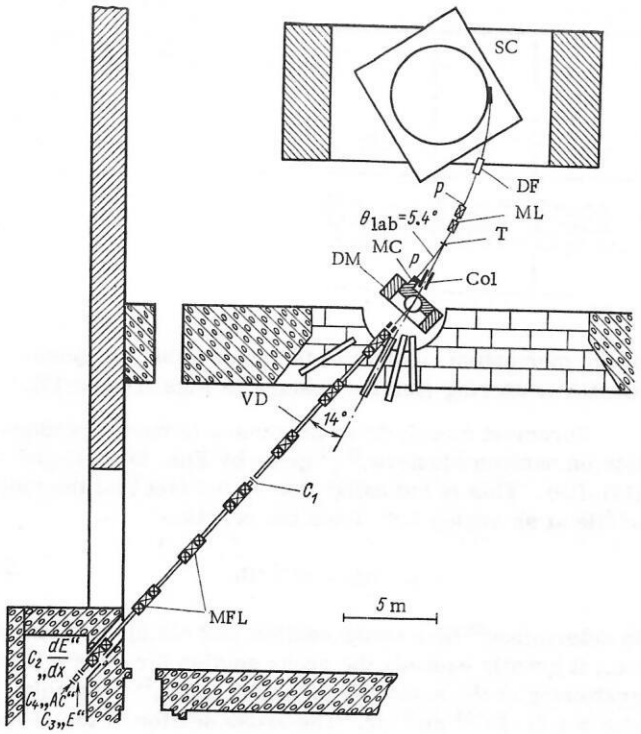

Fig. 17. General diagram of experiments[19-21] and arrangement of apparatus: SC) synchrocyclotron; DF) deflecting equipment; p) extracted proton beam; T) target; MC) monitoring chamber; Col) collimators; DM) deflecting magnet; VD) vacuum duct; C_1-C_4) scintillation counters; ML) magnetic lens; MFL) magnetic focusing lens.

nuclei theoretical estimates of the effective number of α clusters.[22,23] Experiments on the knock-out of ^{3}He were carried out with ^{6}Li, ^{9}Be, ^{12}C, and ^{16}O as targets. In the first experiments they studied the contribution of the He nuclei in the highest-energy spectral region kinematically accessible at T_p = 665 MeV, namely $T_{^3He}$ = 400-600 MeV and $T_{^4He}$ = 390-550 MeV.

The measurements have shown that in interaction of protons with light nuclei, the yield of fast ^{3}He nuclei observed in the indicated energy interval exceeds by more

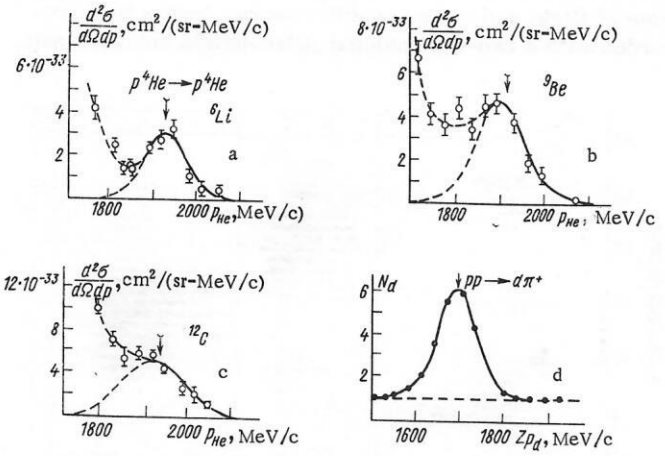

Fig. 18. Yield of fast ^{4}He nuclei from ^{6}Li, ^{9}Be, and ^{12}C at an angle 5.4° to the proton beam, B_p = 665 MeV (a-c): The arrow indicates the momentum of the ^{4}He nuclei following elastic p^4He scattering ($p_{^4He}$ = 1923 MeV/c, $T_{^4He}$ = 467 MeV); d) yield of deuterons (in relative units) from CH_2 target in the immediate vicinity of the effective momentum used to calibrate the He-yield cross sections.

than one order of magnitude the yield of ^{4}He nuclei (Figs. 18 and 19). A characteristic feature of the spectra is a peak in the yield of He from ^{6}Li (ref. 6) and a less clearly pronounced one in the yield from ^{9}Be. In the nuclei ^{12}C and ^{16}O under conditions of ~ 6% momentum resolution one observes only a certain nonmonotonicity in the He spectra. The observed increased yield of the knocked-out nuclei can be naturally attributed to the contribution of direct reactions, whose kinematics is close to the kinematics of two-particle reactions with production of the He nucleus in the final state. In the production of ^{4}He, in addition to scattering by the α-particle clusters

$$p + [^4He] \to p + {}^4He \qquad (8)$$

it is possible in principle to have also the following direct proton–cluster interaction reactions:

$$p + [^3He] \to \pi^+ + {}^4He; \qquad (9)$$
$$p + [^3H] \to \pi^0 + {}^4He; \qquad (10)$$
$$p + [3n] \to \pi^- + {}^4He; \qquad (11)$$
$$p + [^3H] \to \gamma + {}^4He; \qquad (12)$$
$$p + [^4H] \to n + {}^4He; \qquad (13)$$
$$p + [^6Li] \to {}^3He + {}^4He. \qquad (14)$$

However, the momentum of ^{4}He from reactions (9)-(11) is 1600 MeV/c, and that from reaction (12) is 1620 MeV/c, i.e., much lower than in the investigated section of the spectrum. The maximum value of $P_{^4He}$ can be reached in the reactions p + (z, A) → (z − 2, A − 4) + ^{4}He. In particular, the momentum of ^{4}He from (14) on a free Li nucleus is 2100 MeV/c and is at the limit of the investigated section of the spectrum.

Thus, the peak in the ^{4}He spectrum at an approximate momentum 1920 MeV/c can be due only to reactions of quasielastic scattering of protons by four-nucleon clusters, (8) and (13). Since the binding energies of the nucleons in a group of the type ^{4}He is much larger than in a group of the type ^{4}H, it should be assumed that the α-particle clusters are spatially more compact than clusters of the

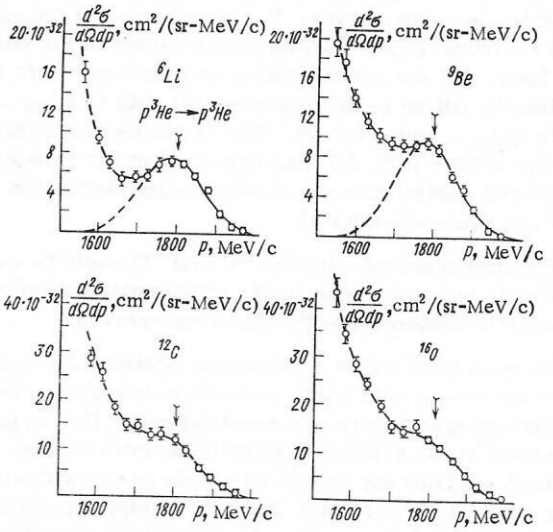

Fig. 19. Yield of fast ^{3}He nuclei at 5.4° to the proton beam, T_p = 665 MeV: The arrow indicates the momentum of the nuclei in elastic p^3He scattering ($p_{^3He}$ = 1803 MeV/c, $T_{^3He}$ = 528 MeV).

TABLE 8

Target nucleus	$\frac{d\sigma}{d\Omega}(p, N^3\mathrm{He})$, 10^{-29} cm^2/sr	$n_{^3\mathrm{He}}$	$\frac{n_{^3\mathrm{He}}}{A/3}$	$\frac{d\sigma}{d\Omega}(p, N^4\mathrm{He})$, 10^{-31} cm^2/sr	$n_{^4\mathrm{He}}$	$\frac{n_{^4\mathrm{He}}}{A/4}$
^{6}Li	1.26±0.23	2.9±0.7	1.45±0.35	3.6±0.7	0.8±0.2	0.52±0.13
^{9}Be	1.75±0.38	4.1±1.1	1.4±0.4	5.4±1.2	1.2±0.3	0.52±0.13
^{12}C	⩽4.2±0.6	⩽9.6±2.0	⩽2.4±0.5	⩽18.2±3.0	⩽4.0±0.9	⩽1.3±0.3
^{16}O	⩽6.6±1.0	⩽15.3±3.2	⩽2.9±0.6	—	—	—

^{4}H type. The probability of transferring a large momentum to a nucleon group should increase sharply with increasing compactness of the group, and consequently one should expect the bulk of the observed yield of ^{4}He with approximate energy 470 MeV to be determined by quasielastic scattering of protons by the α-particle clusters in the nuclei.

A somewhat more complicated situation occurs in the production of fast ^{3}He nuclei. In this case the following quasi-two-particle direct reactions are admissible:

$$p + [^3\mathrm{He}] \to p + {}^3\mathrm{He}; \quad (15)$$
$$p + [^3\mathrm{H}] \to n + {}^3\mathrm{He}; \quad (16)$$
$$p + [2p] \to \pi^+ + {}^3\mathrm{He}; \quad (17)$$
$$p + [d] \to \pi^0 + {}^3\mathrm{He}; \quad (18)$$
$$p + [2n] \to \pi^- + {}^3\mathrm{He}; \quad (19)$$
$$p + [d] \to \gamma + {}^3\mathrm{He}; \quad (20)$$
$$p + [^4\mathrm{He}] \to d + {}^3\mathrm{He}, \quad (21)$$

and also reaction (14). A kinematic analysis analogous to that carried out for the knock-out of deuterons in ^{4}He shows that the main contribution to the yield of ^{3}He with approximate energy 530 MeV should be made by reactions (15) and (16) of quasielastic scattering by three-particle clusters. At the same time, one cannot exclude the possibility of a small contribution from reaction (21), which produces ^{3}He with a momentum 60 MeV/c higher than in (15).

The high-energy sections of the spectra were approximated by Gaussian curves. In the reduction of the spectra of He from ^{6}Li and ^{9}Be, the mean values of the curves were fixed, and the normalization and variance were determined by fitting to the experimental data at $p_{^3\mathrm{He}} > 1780$ MeV/c ($p_{^4\mathrm{He}} > 1900$ MeV/c). The cross-section data presented in Table 8 (ref. 21) take into account the possibility of a 30-40% contribution from other processes in the part of the spectrum considered.

The data obtained with the ^{12}C and ^{16}O could be used to estimate only the upper limits of the contribution of the quasielastic scattering to the observed spectra.

As seen from Table 8, the cross sections for quasielastic knock-out with large momentum transfer to the clusters are quite small and constitute a negligible part of the total cross section of the inelastic interactions. Thus, the cross sections for knock-out of ^{4}He nuclei with energy in the interval 450-470 MeV from ^{12}C nuclei amount to 10^{-6} of the total cross section for inelastic interaction of protons with carbon at 665 MeV. The competing processes increase sharply the yield of He even with a 10% decrease of the momentum relative to the mean value for quasielastic scattering (see the spectra in Figs. 18 and 19).

Foremost among these processes is meson production on nucleon clusters,[12,21] given by Eqs. (9)-(11) and (17)-(19). This is indicated also by the fact that the yield of ^{4}He at an angles 5.8° from the reaction

$$p + {}^3\mathrm{He} \to \pi^+ + {}^4\mathrm{He} \quad (22)$$

is determined[24] by a cross section $(3.3 \pm 1.3) \cdot 10^{-30}$ cm^2/sr, i.e., it greatly exceeds the cross section for elastic p^{4}He scattering at the same ^{4}He detection angle,[25,26] namely $(4.6 \pm 1.2) \cdot 10^{-31}$ cm^2/sr. The cross section of the reaction

$$p + d \to \pi^0 + {}^3\mathrm{He}, \quad (23)$$

which is[24] $(2.0 \pm 0.2) \cdot 10^{-29}$ cm^2/sr, also exceeds appreciably the cross section of elastic p^{3}He scattering,[26] $(4.3 \pm 1.0) \times 10^{-30}$ cm^2/sr. If the ratio of the cross sections of the quasielastic processes to the processes of meson production on clusters has the same character, then we can expect the yield of ^{3}He nuclei with momentum near 1500 MeV/c and of ^{4}He near 1600 MeV/c to be due to a considerable degree to the processes (17)-(19) and (9)-(11), respectively.

The spectra of ^{3}He and ^{4}He were measured in a wider energy interval than in the earlier studies by O. V. Savchenko et al.[21] While the general experimental setup remained the same in these measurements, the data on the particle time of flight and on the specific energy losses were recorded with a two-dimensional pulse-height analyzer and

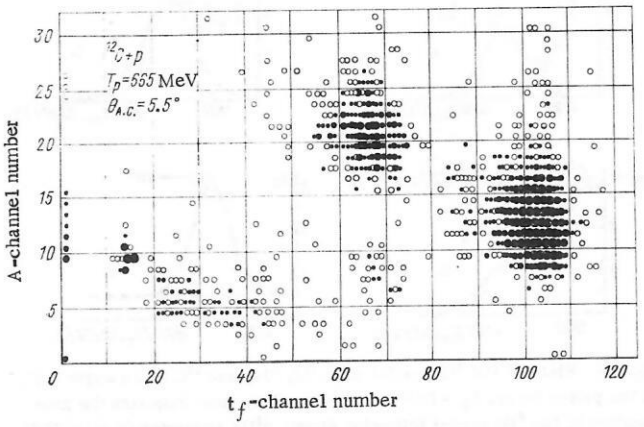

Fig. 20. Two-dimensional spectrum (time of flight vs specific energy loss) illustrating the conditions under which the nuclei ^{3}He and ^{4}He were detected in the experiment of ref. 21.

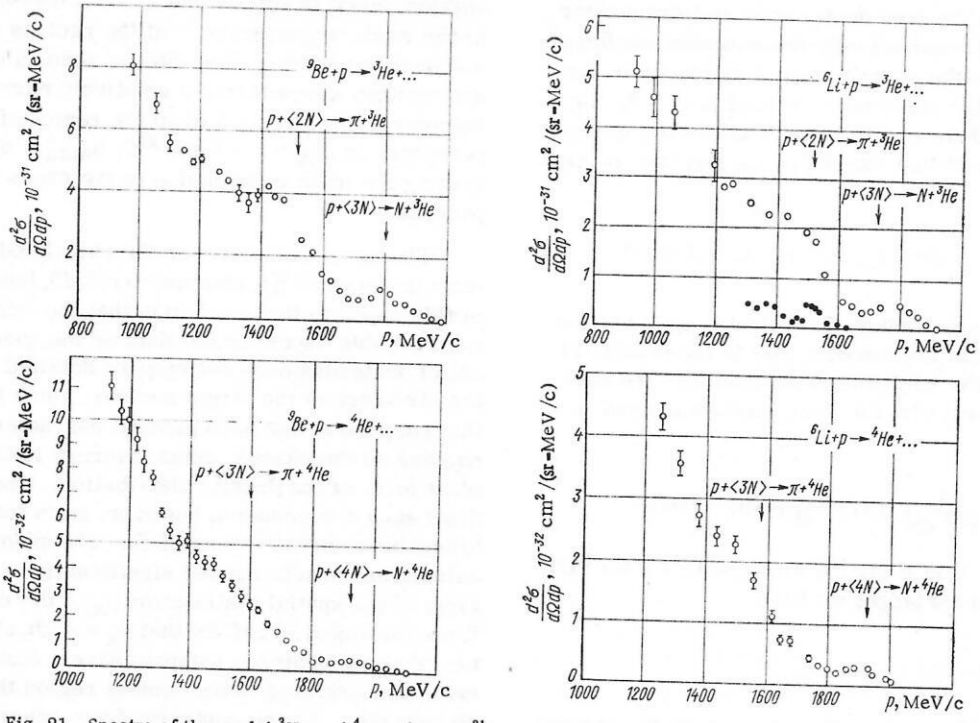

Fig. 21. Spectra of the nuclei ^{3}He and ^{4}He, observed[21] at an angle 5.4° to a proton beam of energy 665 MeV.

analyzed with a computer connected on-line with the apparatus. This has made it possible to measure simultaneously the ^{3}He and ^{4}He spectra with reliable identification of the nuclei (Fig. 20). The absolute values of the cross sections were calibrated in ref. 21 against reaction (7) with allowance for all the known published data on this reaction (see refs. 15). In earlier studies, only the cross sections from ref. 27 were used.

The measurement results shown in Fig. 21 demonstrate that in the spectral region kinematically corresponding to the processes of meson production on clusters there is indeed observed an appreciable increase of the yield in comparison with the quasielastic-peak region. In the He spectra, however, the meson-production process is not as clearly pronounced as in the meson-production process on the nucleons of the nucleus in the deuteron spectra. To determine finally the contribution of the processes of meson production on clusters, it is necessary to perform experiments with direct detection of the He nuclei and pions in coincidence. Such experiments, in conjunction with kinematically complete experiments on the detection of quasielastic knock-out, uncover interesting possibilities for a direct investigation of nucleon clusters.

Particularly attractive is the study of neutron clusters [channels (11) and (19)] that are difficult to investigate by other methods, and also the comparison of information on clusters of a definite type in different reactions. An example of such a possibility is the investigation of the reactions $p + [2n] \to \pi^- + {}^3He$ and $p + [2n] \to n + d$.

2. INTERPRETATION OF EXPERIMENT

A theoretical interpretation of the experiments on the knock-out of fast deuterons by high-energy protons was initiated by D. I. Blokhintsev.[28] The results of experiments[6] on the knock-out of deuterons at 670 MeV were attributed in that reference to direct quasifree interaction of the incident proton with two nucleons in the nucleus. The cross section of such an interaction, according to ref. 28, depends significantly on the probability $W_d(R)$ of finding the neutron and proton in the ground state of the target nucleus at a small relative distance. The absorption of the knock-out deuterons in the cluster matter was estimated in a quasiclassical approximation. It was assumed that the deuteron knock-out from the momentum interval corresponding to quasielastic kinematics is determined by the total cross section for interaction of the deuteron with the nucleons of the nucleus. This concept was developed in ref. 28 for the knock-out of not only deuterons but also of fragments with arbitrary numbers of nucleons. Subsequently, the idea of direct interaction of the incident nucleon with a group of nucleons of the nucleus served as a basis of all the calculations undertaken for a quantitative explanation of quasielastic knock-out of fast fragments. The calculations of B. N. Kalinkin and V. L. Shmonin[29,30] are a direct continuation of the approach developed in ref. 28.

Kalinkin and Shmonin made an attempt to estimate the cross sections for quasielastic knock-out of deuterons, by using the simplest concepts concerning the nuclear structure. Unlike ref. 28, the question of the mechanism of a large momentum transfer to a nucleon system that is bound in the final state was not discussed in refs. 29 and 30, since an identical mechanism was assumed for the scattering by two-nucleon clusters and for pd scattering. This assumption is justified by the fact that the scattering with high momentum transfer is determined by the behavior of the wave function of the np system at small relative distances between the nucleons. Thus, in backward pd scattering at a proton energy $T_p = 1$ GeV, the characteristic distances are of the order of $R \lesssim 0.5$ F. It can be assumed that the behavior of the wave function of the np system at distances much shorter than the average internucleon distance in the nucleus ($\bar{r}_{NN} \approx 1.8$ F) changes

little on going from the free deuteron to an intranuclear np pair. Taking into account only the renormalization of the wave function of the np pair when it is placed in the nucleus, the following expression is used in ref. 29 for the ratio n_d of the differential cross sections for quasielastic deuteron knock-out $(d\sigma/d\Omega)_{(p, pd)}$ and free pd scattering $(d\sigma/d\Omega)_{pd}$:

$$n_d = (d\sigma/d\Omega)_{(p, pd)}/(d\sigma/d\Omega)_{pd} \approx \frac{4}{3}\pi\bar{r}_d^3 \cdot Nz \int d^3r\rho^2(r). \qquad (24)$$

Here $\bar{r}_d$ is the average radius of the deuteron; Nz is the number of pd pairs in the nucleus; $\rho(r)$ is the density of the distribution of the nucleons in the nucleus. To calculate n_d, the function $\rho(r)$ for light nuclei was used in the form

$$\rho(r) = \frac{4}{\pi^{3/2} \cdot a_0^3 A} \cdot \left(1 + \delta \frac{r^2}{a_0^2}\right) \exp\left(-r^2/a_0^2\right)$$

[$\delta = (A-4)/6$, $a_0 = 1.59$ F for ^{12}C and $a_0 = 1.77$ F for ^{16}O], and in the case of a Pb target we have

$$\rho(r) = \frac{\rho_0}{A}\left[1 - \exp\left(\frac{r-c}{a}\right)\right]^{-1},$$

where $\rho_0 = 0.137$ F^{-3}, c = 6.98 F, and $a = 0.55$ F. The values of n_d obtained are listed in Table 9.[29]

Comparison of the calculated and experimental data shows that a calculation without allowance for the distortions overstimates n_d by a factor ranging from 10 for light nuclei to 100 for heavy ones. To take into account the interaction of the incident protons and of the knock-out deuterons with the nucleons of the nucleus, an interaction that takes the knock-out events out of the quasielastic channel, the high-energy approximation of straight-line trajectories was used in ref. 29. The integration in (24) could then be carried out over the impact parameter b and the running coordinate z, with weights $\tau(b, z)$ and $\eta(b, z)$, where

$$\tau(b, z) = \exp[-\sigma T_-(b, z)] \qquad (25)$$

is the probability that a proton with impact parameter b will reach the point z wihout experiencing interaction with the nucleons, and

$$\eta(b, z) = \exp[(-2\sigma + \sigma^2/8\pi a) T_+(b, z)] \qquad (26)$$

is the probability that the deuteron will emerge without interacting with the nucleons of the nucleus; T_- and T_+ in (25) and (26) are given by the integrals

$$T_-(b, z) = \int_{-\infty}^{z} \rho(b, \xi)\, d\xi \text{ and } T_+(b, z) = \int_{z}^{\infty} \rho(b, \xi)\, d\xi \ ;$$

and σ is the total cross section of the NN interaction. The quantity a in (26) determined the dependence of the NN scattering on momentum tranfer, and was assumed to be 7 (GeV/c)$^{-2}$ for an energy 0.7-1.0 GeV. The value of n_d obtained in this manner (see Table 9) agrees within 30% with the experimental data. These calculations show convincingly the need for correct allowance for the distortion of the wave of the incident protons and of the knock-out deuterons when it comes to describing the absolute values of the quasielastic knock-out cross sections. In particular, the $A^{1/3}$ dependence of the knock-out cross section, noted in refs. 7 and 11, is a direct consequence of the weak "transparency" of the nucleus for the proton and deuteron waves. The intense absorption of the incident and emitted waves forms a relatively narrow impact-parameter interval (~ 1.5 F) in the region of the nuclear periphery ($b_{max} \approx 1.8$ F for ^{12}C, $b_{max} \approx 6.7$ F for ^{208}Pb), making the main contribution to the cross section of the process.

The agreement between the calculated and experimental values of $\tilde{n}_d$, obtained in ref. 29, leads the authors of this paper to the conclusion that the interpretation of the available experimental data on the quasielastic knock-out of deuterons does not require detailed information on the structure of the target nucleus, since it suffices for this purpose to use such general characteristics of the nucleus as the charge, mass, average radius, and the simplest form of the density distribution. One can hardly draw such a conclusion, however, from the agreement obtained between the values of $\tilde{n}_d$. The point is that the calculation results depend significantly on the assumed form of the spatial distribution ρ_x of the cluster density. It was assumed in ref. 29 that $\rho_x = \rho^2(b, z)$ for deuterons, i.e., that the deuteron clusters have a distribution that is more concentrated in the central region than the nucleon distribution. To the contrary, from general considerations one can expect the clustering to be more pronounced in the peripheral region of the nucleus, and this is confirmed by quantitative calculations performed in the nuclear-cluster model.[31]

In ref. 14 calculations analogous to those of ref. 29 were carried out for $\rho_x = \rho^2$ and $\rho_x = \rho$. The absolute values

$$\gamma = \frac{\int d^2b\, dz \rho_x(b, z)\, \Gamma(b, z)\, \eta(b, z)}{\int d^2b \cdot dz \cdot \rho_x(b, z)} \qquad (27)$$

increase appreciably in the second case (by approximately a factor of 2 for the ^{12}C nucleus). Agreement is then obtained between the calculated and experimental values of n_d if one uses the total effective number of deuteron clusters obtained within the framework of the shell model[22,32] and account is taken of the contribution of two-nucleon clusters of the (nn) and $(np)_{S=0}$ type.

The relative variation of γ with energy depends little on the form of ρ_x, and is shown in Fig. 22 for $\rho_x = \rho^2$ and $\rho_x = \rho$. We see that in the interval T_p = 380-1000 MeV the value of γ changes in a range of 20% for Li and 26% for C. It follows therefore from the experimentally observed constancy of the ratio $(d\sigma/d\Omega)_{(p, Nd)}/(d\sigma/d\Omega)_{pd}$ (see Fig. 12) that the energy dependence of the cross section for backward scattering of protons by two-nucleon

TABLE 9

Target nucleus		^{12}C	^{16}O	^{208}Pb
$T_p = 1$ GeV	n_{dexp} [7]	5.0±0.5	6.9±1.0	19±2.5
	n_{dcalc}	57.5	71.0	1060
	$\tilde{n}_{dcalc}$	3.7	6.8	17.5
$T_p = 0.675$	n_{dexp} [6]	7±2.5	8±2.5	—
	$\tilde{n}_{dcalc}$	4.1	7.6	

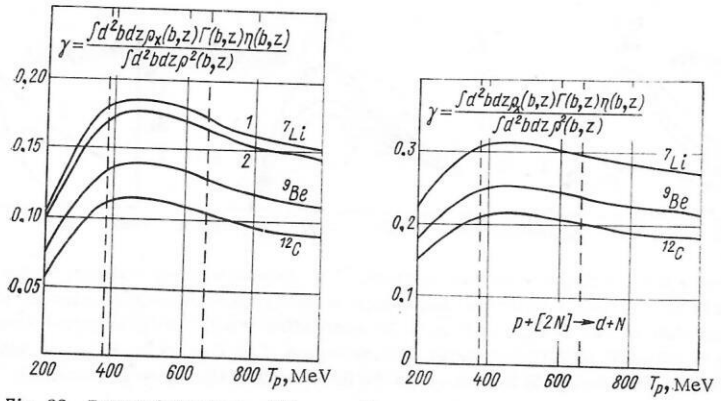

Fig. 22. Energy dependence of the quantity γ, which characterizes the distortion effects in deuteron production reactions.[14]

clusters, accompanied by production of fast deuterons, coincides in the indicated energy interval, within about 30%, with the energy dependence of the elastic backward pd scattering. The distortion of the wave is likewise not changed noticeably when the deuteron detection angle is varied in the range $\theta_d \approx 5$–$15°$. On the basis of the experimental data,[7,11] an analogous conclusion can therefore be drawn also with respect to the angular distributions in quasielastic scattering.

The methods of the dispersion theory of direct nuclear reactions[33] were first used for analysis of deuteron spectra in ref. 34. The spectrum of the deuterons[6] emitted at an angle 7.6° was calculated in the pole approximation with respect to the variable

$$t=-(\bar{p}_A-\bar{p}_B)^2+2(m_A-m_B)(E_A-E_B), \tag{28}$$

which has a pole at the value

$$t_0=2m_d(m_A-m_B-m_d). \tag{29}$$

Here $\bar{p}_A$, $\bar{p}_B$, E_A, and E_B are the momentum and kinetic energies of the nuclei A and B; m_i is the mass of the i-th particle participating in the reaction (Fig. 23). If the nucleus A is at rest prior to the collision, then

$$t=-(m_A/m_B)\,p_B^2. \tag{30}$$

The amplitude of the direct process is larger, the closer the value of t to the pole. One should therefore expect the pole mechanism to be significant in the region of deuteron clusters corresponding to small momenta of the residual nucleus, i.e., where the kinematics of the process is closest to the kinematics of the elastic pd scattering. Outside this region, the other more complicated diagrams can provide the main contribution.

In the pole approximation, the cross section of the process is

$$d\sigma=\text{const}\frac{|\Gamma(p_B)|^2|M(s',t')|^2}{\left(t_0+\frac{m_A}{m_B}p_B^2\right)^2}d^3p_Bd^3p_dd^3p_f$$
$$\times\delta(\bar{p}_B+\bar{p}_d+\bar{p}_f-\bar{p}_i)\,\delta(\mathcal{E}_B+\mathcal{E}_d+\mathcal{E}_f-\mathcal{E}_i), \tag{31}$$

where $\mathcal{E}_a$ is the total energy of the particle with momentum p_a; $\Gamma(p_B)$ is the vertex part (form factor) corresponding to the decay A → B + d; M(s', t') is the amplitude of the elastic scattering at the point $s'=(P_i+P_d)^2$, $t'=(P_f-P_i)^2$ (P_i, P_d, and P_f are, respectively, the 4-momenta of the incident proton, the deuteron, and the proton in the final state). In agreement with Eq. (31), the angular dependence of the knock-out cross section and the dependence of the energy of the incident protons should be determined essentially by the elastic-scattering amplitude M(s', t'). Assuming that M(s', t') is constant in the variable range of interest to us, and replacing the form factor $\Gamma(p_B)$, which does not depend on p_B, by the reduced vertex part, we can roughly account for the form of the spectrum in the region of the quasielastic peak. The calculated curves shown in Fig. 24 for the ground state and for several excited states of the residual nucleus are normalized to the experimental curves at the maximum of the quasielastic peak. The straight lines in Figs. 24a and 24b indicate the momentum of the deuterons from elastic pd scattering. This result demonstrates well the dependence of the form of the spectrum on the excitation of the residual nucleus. Since the excitation spectrum is not calculated within the framework of dispersion theory, it was assumed arbitrarily that the constants of the decay A → B + d to the ground and excited states are equal. The contribution to the reaction cross section from each of the excited states is in this case smaller than the contribution of the ground state, since the pole denominator increases with increasing excitation of the residual nucleus.

The calculations in the pole approximation account correctly for the spectrum only in the region of small t, i.e., only in that kinematic region where the virtual deuteron is emitted with a small momentum. Such deuterons are predominantly outside the potential well of the nucleus,

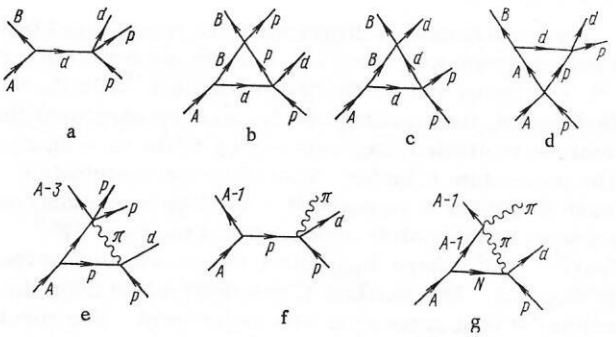

Fig. 23. Diagrams of the dispersion theory of direct nuclear reactions, used in calculation of the deuteron spectra.

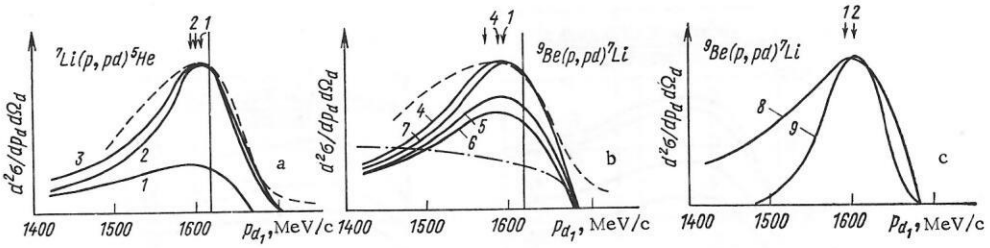

Fig. 24. Momentum spectra of deuterons, calculated[34] by dispersion-theory methods, for the conditions of the experiment in ref. 6: dashed curves – experimental: a and b) calculated without allowance for the form factor; 1) ground state of ^{5}He; 2) 16.7-MeV level; 3) contribution of both levels; 4) ground state of ^{7}Li and 0.48-MeV level; 5) 4.6-MeV; 6) 7.38-MeV level; 7) contribution of all four levels; 8) ground state of ^{7}Li without allowance for the form factor; 9) the same with the form factor of the ^{9}Be → ^{7}Li + d vertex.

and the wave function of their motion relative to the residual nucleus leads to a form factor of the Butler type, determined by the radius R of the nucleus, by the parameter

$$k = \frac{1}{\hbar}\sqrt{2m_{Bd}(m_B + m_d - m_A)}, \qquad (32)$$

which depends only on the particle mass, and by the angular momentum l with which the virtual deuteron is emitted. The change of the calculated spectrum following introduction of such a form factor is seen in Fig. 24c, where the results of calculations without and with a form factor (l = 0) are compared for the reaction ^{9}Be (p, pd) ^{7}Li.

These results show that while the calculation accounts for the shape of the spectrum, it cannot claim an exact description until additional information of spectroscopic character, concerning the probabilities of the virtual emission of a deuteron with a given angular momentum and a definite excitation of the residual nucleus, is introduced. From the point of view of the present authors, who have developed the dispersion-theory method, the problem is to separate correctly that part of the process which corresponds to the concrete mechanism of the reaction (to a definite diagram), and to obtain from comparison with experiment the values of the reduced widths for virtual emission of the clusters by the target nucleus for given states of the residual nucleus. These quantities are characteristics of the nuclei, depend on their internal structure, and do not depend on the type of reaction and on the kinematic conditions under which they were obtained. Thus, from the experimental data[6] on the reduced vertex part of the process ^{9}Be → d + ^{7}Li, an estimate of 0.5-1.0 was obtained in ref. 34. The same quantity should enter into the cross sections of other direct processes with emission of virtual or real deuterons [for example the reaction ^{9}Be(t, n)^{11}B, etc.].

The contribution of diagrams more complicated than the pole diagram was taken into account approximately by V. M. Kolybasov and N. Ya. Smorodinskaya.[35] Unlike the pole diagram, the amplitude of the process corresponding to more complicated diagrams varies little as a function of the momentum transfer. Therefore the contribution of such diagrams is replaced in ref. 35 by a constant, and the square of the matrix element takes the form $|M|^2 = |M_{pol}|^2 + |C|^2$, where M_{pol} is the matrix element of the pole diagram. The constant C was determined from the condition of best agreement with experiment. The results of such a calculation, given in Fig. 25, show that for the reaction ^{4}He (p, pd) at 1 GeV energy the contribution of diagrams other than the pole diagram can be neglected, and in the case of the reaction ^{16}O(p, pd) the value of C at small momentum transfers has an absolute value approximately equal to 1/15 of the entire amplitude. The combined deuteron width for the reaction ^{4}He(p, pd) proceeding with production of a slow deuteron as a residual nucleus or with emission of an unbound np pair was estimated at 9.0 ± 2.0. For the reaction ^{16}O (p, pd) ^{14}N, the deuteron width summed over the states of ^{14}N with excitation energy ≤ 5 MeV was found to be $\sum_i \theta_i^2 = 4.7 \pm 1.0$.

The quality of the description of the spectra following introduction of Butler form factors can be assessed also from the results of ref. 13 (see Fig. 10, where the theoretical curves are shown dashed). It is important that the values of the reduced widths obtained in that reference for the reaction ^{12}C(p, pd) turn out to be close within the

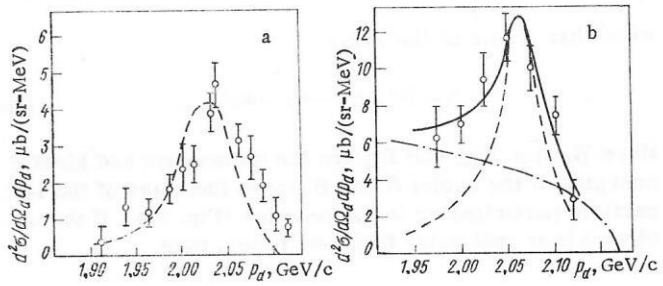

Fig. 25. Calculation[35] of the momentum spectra of the deuterons emitted at T_p = 1 GeV in the following reactions: a) ^{4}He (p, pd)^{2}H, θ_d = 10.1°; b) ^{16}O (p, pd)^{14}N, θ_d = 4.38°. The experimental points were taken from ref. 7.

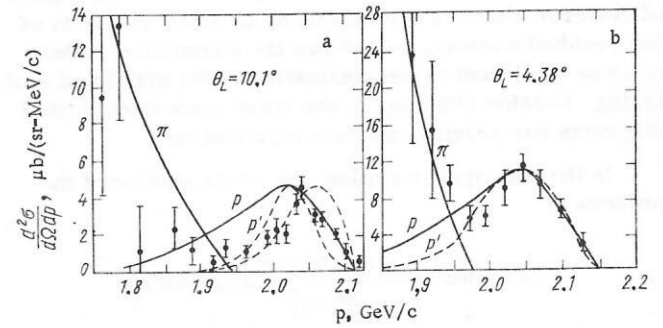

Fig. 26. Calculated spectra of deuterons[36] for the reactions: a) ^{4}He (p, pd)^{2}H; b) ^{16}O(p, pd)^{14}N; p' and p describe the contribution of the pole diagram (see Fig. 23a) with and without the form factor, respectively, for the decay vertex; T' describes the contribution of the triangular diagram (see Fig. 23b) with the form factor included; π) (p, πd) generation in accordance with the diagram of Fig. 23f.

TABLE 10

Nucleus	^{7}Li	C	Al	Cu	Rh	Pb
0_d^2	2.4±0.5	4.4±0.8	7.4±1.4	8.6±1.6	10.3±2.0	12.6±2.5

limits of the experimental accuracy:

$$0_d^2 = 3.8 \pm 1.0 \quad \text{for} \quad T_p = 1260 \text{ MeV}$$

and

$$0_d^2 = 2.7 \pm 0.7 \quad \text{for} \quad T_p = 730 \text{ MeV}$$

even though the cross sections in the quasielastic maximum of the spectra differ at these values by an approximate factor of 5.

The theoretical curves shown in Fig. 7 in the region of the quasielastic peak of the deuteron spectra[11] were also obtained with the aid of the dispersion-theory method. A pole diagram was used (see Fig. 23a) without allowance for the form factor and for the excitation of the residual nucleus. To calculate the reduced widths θ^2_d of the decay A → B + d, a Butler form factor was chosen in the vertex part ($l_d = 0$). The results of a calculation in which the experimental data were used for $\theta^2_d = 6.5°$ are shown[11] in Table 10. It is important that the values of θ^2_d obtained for other angles coincide within the limits of errors with these values. The curves describing the softer part of the spectrum in the same figures were obtained by using the diagram for meson production on the nucleons of the nucleus in the pole approximation (see Fig. 23f) and with allowance for the diagrams of pion rescattering by the residual nucleus (see Fig. 23g).

Analysis of the experimental data at 1 GeV (ref. 7) with allowance for more complicated diagrams was carried out in ref. 36. Following ref. 34, the authors have also assumed that the square of the off-mass amplitude for proton scattering by a virtual deuteron is constant in the integration region and is proportional to the corresponding cross section of free pd scattering, while the form factor $\Gamma(p_B)$ was assumed to be either constant or in Butler form. It was assumed, in accordance with the results of ref. 22, that the angular momentum l for the emission of a deuteron relative to the residual nucleus for ^{4}He is for the most part equal to zero, while emission of deuterons with $l = 2$ predominates for ^{16}O. Whereas satisfactory agreement with experiment was obtained for ^{16}O, in the case of ^{4}He the maximum value of the deuteron yield is reached at momenta somewhat lower than in the experiment (Fig. 26). It was found that the diagram of Fig. 23b, which describes the interaction of a proton with a residual nucleus in the final state, leads to deuteron spectra with a peak shifted to the right relative to the experimental value. The remaining investigated triangular diagrams (see Figs. 23c, d, e) yield spectra with maximum yield at much lower momenta. For heavier targets than ^{4}He, the cross section maximum calculated from the diagram of Fig. 23b occurs at momentum values quite close to those given by the pole diagram, and therefore the contribution of such a triangular diagram is not noticeable.

It should be noted that the conclusion drawn in ref. 35, that rescattering effects have a relatively weak influence, does not contradict the conclusions considered above, that these processes exert an appreciable influence on deuteron knock-out. The difference betweeen the conclusions, which seems striking at first glance, stems from different definitions of the knock-out process. In the quasiclassical approach or in the impulse approximation it is assumed that the proton can be scattered by intranuclear quasideuteron pairs, which can be created dynamically and decay in the entire volume of the nucleus, including its central region. The probability of quasielastic scattering by pairs situated in the central region of the nucleus, without violating the quasielastic kinematics, is small, and the contribution of such pairs to the formation of the quasielastic peak is small. The peak is produced predominantly when peripheral np pairs are knocked out by protons, and in such a knock-out the rescattering effects are relatively small.

Dispersion theory starts out from the very outset from the assumption that the scattering occurs on peripheral virtual deuterons and naturally receives a relatively small contribution from diagrams that are more complicated than the pole diagram in the quasielastic-peak region. For an exact separation of the contribution of the pole diagram it does not suffice to have the spectrum form predicted by the pole model coincide with the experimental form. The calculation examples cited above show that this method has a weak sensitivity. On the one hand, the spectra obtained by pole-diagram calculations depend significantly on the structure of the form factor and on the excitation spectrum of the residual nucleus, and on the other hand some of the triangular diagrams result in peaks that are close in the form and in location to the pole peaks. The problems of separating the reaction mechanism were discussed in papers devoted to the dispersion theory of direct nuclear reactions (see, e.g., ref. 33). A systematic investigation of this problem in conjunction with an experimental study of nuclear (π, πp) reactions can be found in the papers of the group of the Institute of Theoretical and Experimental Physics.[37] For the cluster knock-out reactions, there are at present no experimental data sensitive to the mechanism of the reaction (the contribution with respect to the Treiman–Yang angle, with respect to the momentum transfer in the nuclear vertex, etc.). The facts presented above, namely the agreement between the angular and energy dependences of quasielastic knock-out and free scattering, are therefore most weighty arguments in favor of the important role played by the pole diagram.

Another trend in the analysis of quasielastic knock-out reactions is the use of the impulse approximation. Questions concerning the justification of this approach and its applicability limits in the study of cluster knock-out reactions were discussed in a number of papers, particularly by V. V. Balashov.[3,38]

In the plane-wave impulse approximation, the cross section for a knock-out reaction that leaves the residual nucleus in the state f is described by the following equation (see, e.g., ref. 31):

$$\frac{d^2\sigma}{d\mathbf{k}_p\, d\mathbf{k}_x} = K \frac{d\sigma}{d\Omega}(\tilde{E}, \tilde{\theta})\, n_{if}^{\text{eff}} F_{if}(k_x)\, \delta(\Sigma E_f - \Sigma E_i), \qquad (33)$$

where K is the kinematic factor; $\bar{\mathbf{k}}_p$ and $\bar{\mathbf{k}}_x$ are respectively the momentum of the scattered proton and of the knock-

out cluster X; $d\sigma(E, \Theta)/d\Omega$ is the differential cross section for free pX scattering. The scattering angle in the c. m. s. of the particles p and X was defined as the angle between the vector k_i and k_f of the momenta of the colliding particles in the initial and final states. Since the scattering in quasielastic knock-out occurs off the mass shell, the total energy $\tilde{E}$ is determined either from the momenta (k_p, k_x) of the free particles p and X in the final state or from the momentum of the incident proton k_{p0} and the Fermi momentum k_x of the cluster X in the nucleus. In the case when the momentum of the incident particle greatly exceeds the momentum of the Fermi motion of the cluster ($|k_{p0}| \gg |k_x|$), the difference in the values of $|k_i|$ and $|k_f|$ becomes relatively small. This justifies the customarily employed procedure of replacing the cross section for off-mass-shell scattering by a virtual particle by the cross section for the scattering by the free particle X. The accuracy of such a substitution is still unknown. In recent experiments[39] on the ^{6}Li(π, 2p) reaction, data were obtained showing that the cross section for the interaction of a pion with a quasideuteron cluster in $^6\mathrm{Li}\pi^+ + [np] \rightarrow p + p$ and the cross section of the reaction $\pi^+ + d \rightarrow p + p$ at ~ 80 MeV can differ noticeably. Experimental investigations of off-mass interaction of hadrons with clusters are therefore quite pressing at present.

The function $F_{if}(k_x)$ in Eq. (33) is the density of the momentum distribution of the cluster X in the $i \rightarrow f$ channel:

$$F_{if}(k_x) = \left| \frac{1}{(2\pi)^{3/2}} \int_0^\infty \exp(-ik_x R)\, \Psi_{if}(R)\, dR \right|^2. \qquad (34)$$

The wave function $\Psi_{if}(R)$ of the relative motion of the cluster and of the residual nucleus B in the state f is determined by the integral

$$\int \Psi_B^*(\xi_B)\, \Psi_X^*(\xi_X)\, \Psi_A(\xi_A)\, d\xi_B\, d\xi_X = a_{if} \Psi_{if}(R), \qquad (35)$$

where Ψ_A is the wave function of the target nucleus A, Ψ_B is the wave function of the nucleus B, and Ψ_X is the internal wave function of the cluster X. A detailed discussion of questions connected with the determination of the form factors $F_{if}(k_X)$ and of the effective numbers

$$n_{if}^{\mathrm{eff}} = \frac{A!}{(A-X)!\, X!} |a_{if}|^2 \qquad (36)$$

can be found in refs. 22, 23, 31, 32, and 38. The same references give the values of the total effective numbers N_X^{eff}, which are the sums of n_{if}^{eff} over all the permissible states of the final nucleus. The principal results of these calculations, carried out within the framework of the shell model with LS coupling, reduce to the following:

TABLE 11

Target Nucleus	(p, pd)		(p, p ^{3}He)		(p, p ^{4}He)	
	$N_p^{\mathrm{eff}}(d)$	$\frac{N_p^{\mathrm{eff}}(d)}{A/2}$	$N_p^{\mathrm{eff}}(^3\mathrm{He})$	$\frac{N_p^{\mathrm{eff}}(^3\mathrm{He})}{A/3}$	$N_p^{\mathrm{eff}}(^4\mathrm{He})$	$\frac{N_p^{\mathrm{eff}}(^4\mathrm{He})}{A/4}$
^{8}Be	2.95	0.66	1.99	0.66	1.38	0.61
^{10}B	4.17	0.84	1.95	0.55	1.12	0.45
^{11}B	5.01	0.91	3.21	0.88	1.25	0.45
^{12}C	6.69	1.1	—	—	2.37	0.79
^{14}N	8.57	1.2	—	—	2.72	0.78
^{16}O	11.80	1.5	—	—	4.42	1.10

1. The effective numbers of clusters of the type d, ^{3}H, ^{3}He, and ^{4}H knocked out from the p-shell of light nuclei with mass number A are commensurate with the quantity A/X, where X is the number of nucleons in the cluster (Table 11).[22,32]

2. The total effective numbers of d, ^{3}H, ^{3}He, and ^{4}He clusters knocked out from the p and s shells of light nuclei greatly exceed A/X. In particular, N^{eff} (^{4}He) exceeds the value A/4 assumed in the α-particle model. The reason for this is the overlap of the cluster, whereby the exchange of nucleons between them leads to the appearance of exchange amplitudes that increase the reaction cross section. It is seen from Table 12 (refs. 22, 32) that the shell model predicts an appreciable increase of N^{eff} if transitions leading to hole states in the 1s shell are turned on. In addition, it is seen from Table 12 that, according to the calculations, the ability of a nucleon to form clusters decreases on going from the outer shell to the inner s shell. Such a behavior corresponds to the expected spatial distribution of the clusters: The cluster distribution density should be maximal in the surface layer of the nucleus, where the nucleon distribution density is far from saturation. This character of the distribution is customarily attributed to the fact that the influence of the Pauli principle, which suppresses the clustering, becomes more strongly manifest in the central region of the nucleus.

3. The effective numbers of different clusters of the type d, ^{3}H, ^{3}He, and ^{4}He for one and the same nucleus reach values of the order of several units. The effective numbers of heavier clusters have much lower values. It should be noted that the summation of the effective number of clusters of different types has no physical meaning, since the separation of the nucleon clusters of different types corresponds to a quantum-mechanical expansion of the nuclear wave function in terms of different orthonormal bases.

4. The distribution of the probability of the cluster knock-out reaction with respect to the excitation of the residual nucleus has, as a rule, a maximum not for the ground state but for the excited states of the residual nucleus (Table 13). The dependence of the cross section of

TABLE 12

Target Nucleus	N^{eff} (^{4}He) from the configuration nucleons					Total effective numbers						
	p^4	sp^3	s^2p^2	s^3p	s^4	$N^{\mathrm{eff}}(d)$	$N^{\mathrm{eff}}(^3\mathrm{H})$	$N^{\mathrm{eff}}(^4\mathrm{He})$	$N^{\mathrm{eff}}(^6\mathrm{Li})$	$N^{\mathrm{eff}}(^7\mathrm{Li})$	$N^{\mathrm{eff}}(^8\mathrm{Li})$	$N^{\mathrm{eff}}(^8\mathrm{Be})$
^{12}C	2.38	1.90	1.58	0.96	0.40	10.4	11.8	7.2	—	—	—	—
^{16}O	4.44	4.44	3.00	1.39	0.38	15.5	20.4	13.6	0.09	0.13	0.005	0.3

TABLE 13

Nucleus	^{9}Be	^{10}B	^{11}B	^{12}C	^{13}C	^{14}N	^{16}O	
I $l=0$	0.07		0.23		0.20	0.03	0.07	$N^{\text{eff}}(d)$
$l=0;\ 2$	0.58	0.20	0.50	2.33	0.68	0.33	1.84	
II $l=0$	1.03	0.60	1.20	1.41	1.28	0.94	2.00	
$l=0;\ 2$	2.95	4.17	5.00	6.69	9.72	8.57	11.80	
I $l=0$			0.16	0.54	0.41		0.24	$N^{\text{eff}}(^{4}\text{He})$
$l=0;\ 2$	0.53	0.013	0.55	0.54	0.41	0.76	0.24	
II $l=0$		0.18	0.19	0.57	0.23	0.16	0.39	
$l=0;\ 2$	1.38	1.12	1.25	2.37	2.13	2.72	4.42	

Note: I) transitions to the ground state of the residual nucleus; II) sum of transitions to all states s^4p^{n-2} (s^4p^{n-4}).

the reactions of knock-out of the cluster X on the degree of segregation of the clusters in the nucleus has the following qualitative form: In the case of extreme segregation of the clusters (say the α-particle model), the effective number of clusters $N^{\text{eff}}(X)$ is equal to A/X, and the cross section of the reaction is minimal. The maximum value $N^{\text{eff}}(X) = [A!/(A-X)!X!]$ is determined by the pure combinatorics of combining A classical particles into groups of X particles each. The real nuclear system has a value $N^{\text{eff}}(X)$ intermediate between these extreme cases. In particular, allowance for the symmetry properties of the nuclear wave function within the framework of the shell model leads to the appearance of a factor $|a_{if}|^2$ in Eq. (36) and yields the values of $N^{\text{eff}}(X)$ given[32] in Tables 11-13.

A more accurate account of the interaction between the nucleons of different clusters is obtained in the nucleon-cluster model.[31,40-43] This model gives a nucleon-cluster segregation of a type intermediate between the shell model and the cluster model.

The obvious advantages of the foregoing description of the knock-out reactions are its relative simplicity and ordered approach. The equation for the cross sections in the plane-wave impulse approximation take the form of products of factors that depend only on the cluster structure of the nucleus, and factors determined by the "elementary" process of the scattering of the incident particle by the cluster. It is apparently precisely the simplicity of the interpretation which attracts the authors using the plane-wave approximation for analysis of the experimental data, in spite of the fact that the significant role of the distortion of the plane waves by the nuclear potential is well known. Thus, the experimental data on the reaction ^{6}Li (p, pd) ^{4}He were analyzed in ref. 16 in the plane-wave impulse approximation. They utilized the equation

$$\frac{d\sigma(K_X)}{d\Omega_p\, d\Omega_d\, dE_p} = K\left(\frac{d\sigma}{d\Omega}\right)_{pd} n_{\alpha d}\rho(K_X), \tag{37}$$

where $(d\sigma/d\Omega)_{pd}$ was taken to be the cross section for elastic pd scattering through 90° in the c.m.s. The momentum distribution $\rho(K_X)$ obtained in this manner for the deuteron cluster relative to the α cluster in ^{6}Li is shown in Fig. 14. The curve in the figure is the result of the calculations by Yu. A. Kudeyarov et al.[43] In the model developed by these authors for ^{6}Li, the configuration ^{4}He (ground state) d in ^{6}Li has a momentum distribution in the form

$$\rho(K_X) \sim \Big|\sum_{i=0,1,2}(a_i + b_iK_X^2)\exp(-C_iK_X^2)\Big|^2, \tag{38}$$

where only two parameters are free, and their values can be fixed by comparing the calculations with the data on the electromagnetic form factors of ^{6}Li. It is seen from Fig. 14 that the agreement between the theoretical form $\rho(K_X)$ and the experimental data is quite good. The theoretical value of $n_{\alpha d}$ is close to 1.0, and the value of $n_{\alpha d}$ obtained in ref. 16 is 0.8 ± 0.06. Quantitative conclusions can be drawn from this only after the distortions are taken into account, in analogy with the procedure used in ref. 44.

Indeed, an analysis of the ^{6}Li (p, pd) reactions in the plane-wave approximation shows a strong dependence of the data for $\rho(K_X)$ and $n_{\alpha d}$ on the energy at which the reaction is investigated[16] (Table 14). The same data demonstrate well also the advantage of investigating cluster knock-out reactions at energies at hundreds of MeV in comparison with low energies: The experimental value of $n_{\alpha d}$ obtained from Eq. (37) approaches the theoretically expected value only at 590 MeV.

A definite improvement in the analysis methods was undertaken by V. V. Balashov and V. I. Markov,[48] where the data on the (p, Nd) n(p, πd) reactions were analyzed in the strong-cutoff model. To take into account the peripheral character of the reactions, the integration in (34) was carried out not over the entire volume of the nucleus, but

TABLE 14

Energy, MeV	Full width at half maximun for $\rho(K_X)$, MeV/c	$n_{\alpha d}$	Reference
30	42—64	0.04±0,12	[45]
55	64±4	0.15±0,07	[46]
155	68±8	0.31±0,15	[47]
590	124±4	0.80±0,06	[16]

TABLE 15

Nuclear excitation energy, MeV	l_N	n_{if}^{eff}	n_{if}^{act} R_c=2.6 F	$n_{if}^{\text{act}}/n_{if}^{\text{eff}}$
0	1	2.50	1.03	0.41
2.10	1	0.66	0.27	0.41
5.03	1	0.76	0.33	0.44
5.5—20	1	0.08	0.03	0.38
20	0	2	0.34	0.17
*N*eff	—	6	2.00	0.33

TABLE 16

Nuclear excitation energy, MeV	l_d	n_{if}^{eff}	n_{if}^{act} $R_c = 2.4$ F	$n_{if}^{\text{act}}/n_{if}^{\text{eff}}$
0	2	2.33	0.97	0.42
	0	0.36	0.18	0.50
0.7	2	0.40	0.16	0.40
	0	0.91	0.46	0.50
2.1	2	0.05	0.02	0.40
3.5	2	0.72	0.30	0.42
6.1	2	0.49	0.20	0.41
Higher excitations	0	0.13	0.06	0.46
	2	0.85	0.35	0.41
20	1	5.04	1.06	0.21
35	0	1.98	0.13	0.07
	—	13.26	3.89	0.29

over its outer region with $|R| \geq |R_c|$. The distributions of the effective numbers of nucleons and deuterons n_{if}^{eff} over the excitation spectrum of the residual nucleus, employed in the calculations and obtained in refs. 22 and 32, are listed in Tables 15 and 16.[48]

The cross sections of the "elementary" processes (3) and (5) were taken to be the known experimental cross sections of the processes (pd → pd) and (7), respectively. Therefore the only free parameters in the calculations were the independent values of the cutoff radii R_c for the two channels. It turned out that at $R_c = 2.4$ F for channel (3) and $R_c = 2.6$ F for channel (5) it is possible to obtain a satisfactory description of the spectrum in a wide interval of deuteron energies (Fig. 27). The nature of channel (5) is simpler than channel (3), since the process (5) occurs on an individual nucleon and has no direct bearing on the cluster structure of the nucleus. As a result, a simultaneous description of both channels increases the reliability of the conclusions pertaining to the more complicated channel (3). The curves in Fig. 27 differ in the method used to construct the t-matrix of the "elementary" processes off the mass shell: In case 1, the total energy was determined from the momenta $k_p(k\pi)$ and k_d of the free particles, and in case 2 it was determined from the momentum of the incident proton at the Fermi momentum of the nucleon (deuteron) in the nucleus. The slight difference between these curves demonstrates the degree of calculation uncertainty, due to the leeway in the choice of the values of the t-matrix off the mass shell.

Calculation shows the degree to which allowance for the absorption decreases the values of the effective cluster numbers connected with different excitation levels of the residual nucleus (the ratio $n_{if}^{\text{act}}/n_{if}^{\text{eff}}$ in Table 16). We see that the clustering connected with high excitation of the residual nucleus is due to knock-out of the clusters from the internal regions of the nucleus. To determine the spatial distribution of the clusters in the nucleus, experiments are needed with detection of both fast particles (p and d), with an accuracy sufficient to obtain the excitation spectra of the residual nucleus. An analysis of such data should be carried out with the absorption effects taken into account more accurately than in the cutoff model. The calculations in the straight-line trajectory approximation[29,30,14] show the possibility of performing calculations without introducing additional free parameters.

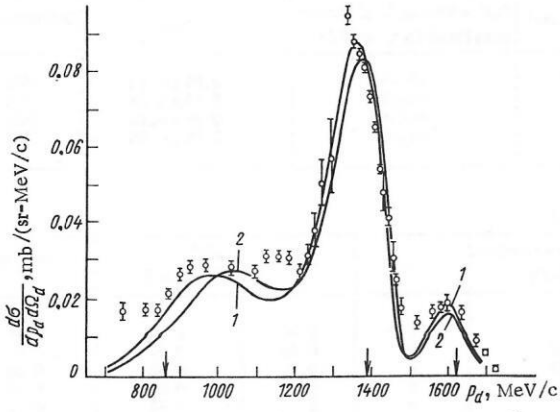

Fig. 27. Results of the description[48] of the deuteron spectrum[10] obtained in the strong-cutoff model.

We turn now to the question of knock-out of fast nuclei that are more complicated than the deuteron. Figure 28 shows the differential cross sections of quasielastic knock-out of deuterons, ^{3}He, and ^{4}He at an approximate proton energy 670 MeV. The figure shows the cross sections for elastic pd, p^{3}He, and p^{4}He scattering with the recoil nuclei detected at small angles in the laboratory frame (the small difference between the angles of observation of the deuterons and the He nuclei is of no importance to the comparison of the cross sections of the processes).

What is most striking is the fact that the fragment-knock-out cross section decreases rapidly with increasing

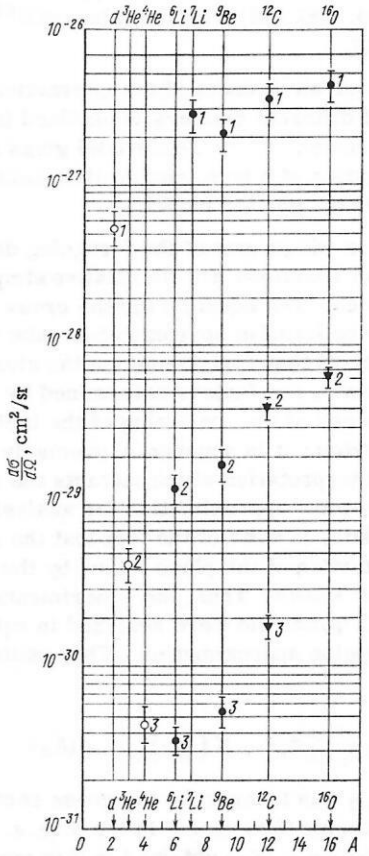

Fig. 28. Differential cross sections for quasielastic scattering of protons with Tp = 665-675 MeV in A(p, NX) reactions and elastic scattering pX → pX at large momenta transferred to the nuclei X: 1) reactions[6] with X = d, $\theta_d = 7.6°$; 2) X = ^{3}He, $\theta^3\text{He} = 5.4°$ (ref. 21); 3) X = ^{4}He, $\theta^4\text{He} = 4.5$ (ref. 21); ○) free pX scattering; ●) quasielastic scattering; ▼) upper limit of quasielastic scattering.

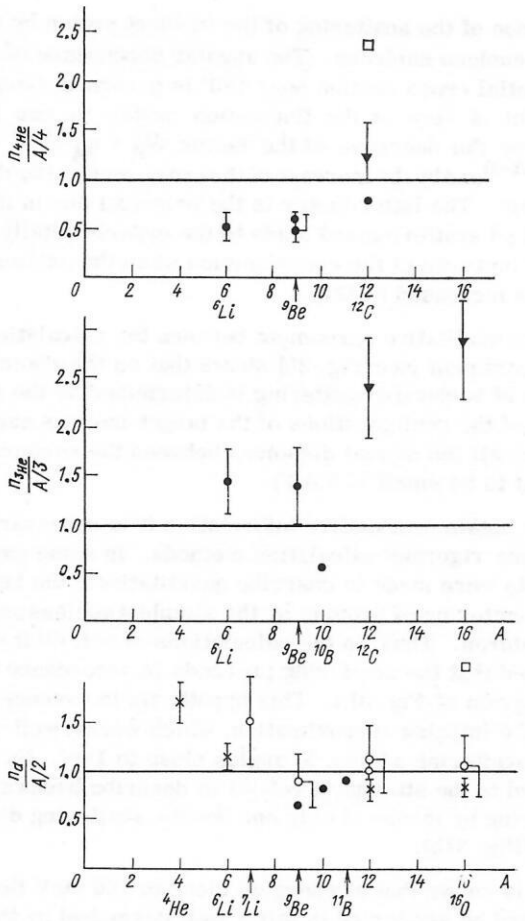

Fig. 29. Ratio n_X of the cross sections of quasielastic scattering A(p, NX) to the cross sections of free pX → pX scattering: ● and ▼) from the data of ref. 21; ○) ref. 6; X) ref. 7; the points shown without error bars are the results of calculations of the effective numbers on the basis of the shell model; ■) ref. 22; □) ref. 23.

mass number of the fragments. Thus, for the target nucleus ^{9}Be the ratio of the yields of ^{4}He, ^{3}He, and deuterons is

$$W_{^4He}:W_{^3He}:W_d = 1:33:4100.$$

At the same time, the ratio of the free-scattering cross sections is

$$\left(\frac{d\sigma}{d\Omega}\right)_{p^4He}:\left(\frac{d\sigma}{d\Omega}\right)_{p^3He}:\left(\frac{d\sigma}{d\Omega}\right)_{dp} = 1:9.4:1200.$$

This correspondence between the cross sections shows that the yield of the fastest fragments is determined primarily by the cross section for elastic scattering of the protons by the nucleon clusters. This confirms qualitatively once more the notion that the quasielastic peaks in the fragment spectra are due to direct quasifree interaction of the incident proton with the nucleon clusters, and the cross sections of this interaction are close to the cross sections for elastic scattering of protons by deuterons, ^{3}He, and ^{4}He, respectively. It is interesting to note that the relative yield of the nuclei ^{3}He and ^{4}He, when these nuclei have energies on the order of hundreds of MeV, differs greatly from the yield observed at low energy of the He nuclei. In the region where the statistical mechanism of fragment production is effective, the emission of ^{4}He is energetically favored, and the yield of ^{4}He at energies 10-20 MeV is larger by one order of magnitude than the yield of ^{3}He (ref. 49).

The ratio of the cross sections for quasielastic knock-out to the free-scattering cross sections, which in the plane-wave impulse approximation have the meaning of the total effective number of clusters, are shown in Fig. 29. For convenience in comparison, these ratios, designated n_X, have been divided by the quantity A/X, where A is the mass number of the target nucleus and X is the number of nucleons in the cluster. It follows from these data that in light nuclei the total effective numbers of two-, three-, and four-nucleon clusters capable of taking on large momentum transfers ($q = 8$–$10\ F^{-1}$), without allowance for absorption effects, are close to the value A/X with an error ~ 1.5-2. The effective numbers of nucleon clusters in the p shell of light nuclei, calculated in the shell model, are of the same order of magnitude. The fact that the observed values of n_X are noticeably smaller than the expected values of the total effective numbers including the clustering of the nucleons of not only the p but also of the s shell indicates in the case of the nuclei ^{3}He and ^{4}He that the knock-out of these fragments has a peripheral character.

3. ELASTIC BACKWARD SCATTERING OF PROTONS BY THE LIGHTEST NUCLEI

The possibility of obtaining information on the short-range correlations between the nucleons making up a cluster from experiments on quasielastic knock-out is based on knowledge of the mechanism of elastic scattering of protons by the lightest nuclei under conditions of high momentum transfer. The amplitude of elastic scattering of hadrons by nuclei at energies 0.2-1 GeV can be expressed with good accuracy in terms of the NN-scattering amplitudes and the wave functions of the nuclei only in the region of small scattering angles θ, and consequently small momentum transfer. The region of intermediate scattering angles is described rather poorly in all the known theoretical approaches. The largest momentum transfers (q_A) are obtained in scattering through 180°. The definitely preferred position of the scattering for which $\cos\theta \approx 1$ gives grounds for expecting the interpretation of the scattering mechanism near 180° to be simpler than at intermediate angles. Let us examine briefly the research aimed at solving this problem.

On the whole, there have been very few studies of backward elastic scattering in the energy region considered. It is known that the main features of this scattering reduce to the following:

1. The cross section of scattering through 180° decreases rapidly with increasing energy as a rule.

2. This decrease of the scattering cross section is faster, the heavier the target nucleus.

3. The angular dependence of the deuteron backward-scattering cross section has a maximum at $\theta = 180°$.

The general picture of the energy dependence of the backward-scattering cross section is shown in Fig. 30, which gives also the results of a calculation[26,55] based on

the fluctuation approach.[28,50] Within the framework of this model, the differential cross section $(d\sigma/d\Omega)_{pA}$ for elastic scattering of a proton by a nucleus with mass number A is estimated from the equation

$$\left(\frac{d\sigma}{d\Omega}(p_A, 180°)\right)_{pA} = \gamma\left(\frac{d\sigma}{d\Omega}\left(\frac{p_A}{A}, 180°\right)\right)_{pN} W_A(R_A), \quad (39)$$

where $(d\sigma/\Omega)_{pN}$ is the differential cross section for elastic pN scattering; $A \leq \gamma \leq A^2$; $W_A(R_A)$ is the probability of finding the nucleons of the nucleus in a spherical region V of radius $R_A \approx \hbar/q_A$. The quantity $W_A(R_A)$ is determined by the integral of the wave function of the nucleus over the volume V:

$$W_A(R_A) = \int_V |\Psi_A(\mathbf{r}_1 \ldots \mathbf{r}_A)|^2 d\mathbf{r}_1 \ldots d\mathbf{r}_A. \quad (40)$$

If it is assumed that Ψ_A varies little in the region of V (at distances $\lesssim 0.5$ F between the nucleons), then the value of $W_A(R_A)$ is proportional to the volume of a 3 (A − 1)-dimensional sphere of radius R_A, i.e., $W_A(R_A) \sim R_A^{3A-3} \sim q_A^{-(3A-3)}$. Since q_A in the energy region considered is connected, with accuracy better than 10%, with the proton energy in the lab by the relation

$$q_A \approx [2A/(A+1)]\sqrt{2m_N T_p},$$

it follows that $W_A \sim T_p^{-(3A-3)/2}$. Inasmuch as the energy dependence of the remaining factors in (39) can be neglected, the backward-scattering cross section should have a similar dependence to first-order. The only free parameter that is common to all the curves of Fig. 30 is the quantity k in the relation $R_A = k(\hbar/q_A)$. Fitting to the experimental data yields a value of k close to unity: k = 1.6. The corridors of the calculated values are determined by the value of γ, which reflects the degree of coherence of the scattering of the incident proton by the target-nucleus nucleons. The angular dependence of the differential cross section near 180° is governed, from the point of view of the fluctuation model, by two factors: by the decrease of the factor $W_A \sim q_A^{-(3A-3)} \sim (\sin\theta/2)^{-(3A-3)}$ and by the increase of the cross section $(d\sigma/d\Omega)_{pN}$ near 180°. The latter factor is the principal one in the case of pd scattering and leads to the experimentally observed increase of the cross section when the scattering angle is increased to 180°.

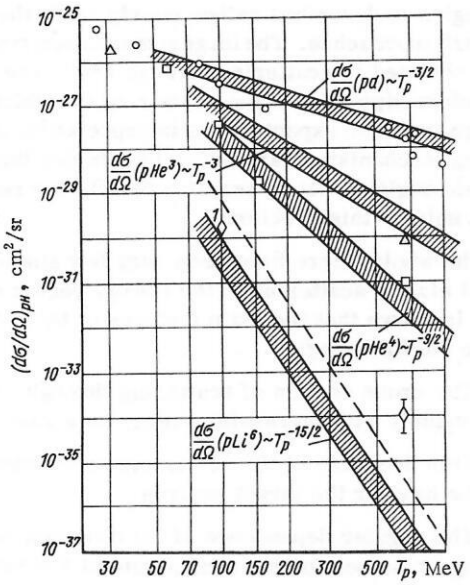

Fig. 30. Elastic backward scattering of fast protons by the nuclei d, ^{3}He, ^{4}He, and ^{6}Li: ○) pd (refs. 51-54); △) p^{3}He (refs. 55, 25, 56); □) p^{4}He (refs. 57, 58, 25); ◇) p^{6}Li (ref. 59); the point for p^{6}Li scattering at T_p = 665 MeV corresponds to the upper limit of the cross section.[55,26]

The qualitative agreement between the calculations and experiment (see Fig. 30) shows that on the whole the picture of backward scattering is determined by the probability of the configurations of the target-nucleus nucleons at which all the mutual distances between the nucleons turn out to be small ($\lesssim 5.0$ F).

To obtain quantitative information it is necessary to use more rigorous calculation methods. In some papers attempts were made to describe quantitatively the backward scattering of protons by the simplest nucleus namely the deuteron. Thus, in the calculations of ref. 60 it was proposed that the scattering proceeds in accordance with the diagram of Fig. 31a. This hypothesis in essence extends the impulse approximation, which works well at small scattering angles, to angles close to 180°. No less justified is the attempt in ref. 61 to describe backward scattering by means of only one double-scattering diagram (Fig. 31b).

It is known that at energies close to 100 MeV the backward pd scattering is fairly well described by the neutron-pickup mechanism (see, e.g., ref. 65). In ref. 52, the experimental data at higher energies were analyzed for the purpose of separating the pole diagram of single-nucleon exchange (see Fig. 31c). In the same reference, the idea was advanced that at high energies and large momentum transfer the nucleon exchange can occur not only in the ground state but also in an excited state. The pole mechanism is singled out because the transferred momenta are in this case much smaller than in direct scattering. Indeed, whereas for direct scattering through 180° the change of the proton momentum is q = 2p (p is the proton momentum in the lab), in the pickup mechanism the change of the proton momentum amounts to only p/2. At an energy T_p = 1 GeV the momentum is p = 5 F^{-1}, and consequently, to realize the pd scattering via the direct-scattering mechanism the deuteron wave function must contain Fourier components corresponding to 10 F^{-1}, as

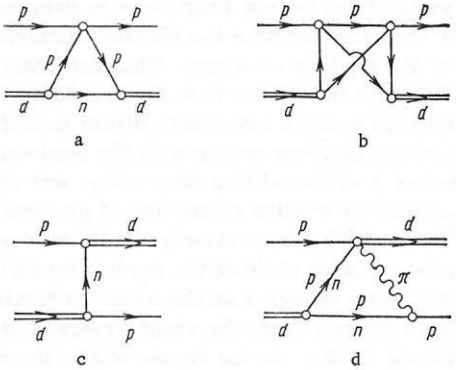

Fig. 31. Diagrams used to describe backward elastic pd scattering.

against only 2.5 F^{-1} for the pickup mechanism.

Since the nucleon–nucleon potentials reach depths on the order of several hundred MeV at distances 0.5–1.0 F, one should expect the effect of nucleon excitation to become significant in backward scattering in the energy region considered. In ref. 63, backward pd scattering was analyzed with allowance for exchange of the N*(1688) baryon resonance with spin 5/2. It was shown that if an admixture of about 1% of a state due to this resonance is included in the deuteron wave function, this will account to approximately one half of the backward-scattering cross section at 1 GeV.

This idea was developed in ref. 66, where, however, no reggeization of the nucleon exchange was employed, and the possible contribution of all the observed N* (I = 1/2) resonances, up to a mass of 2 GeV, was taken into account directly. The authors obtained fair agreement between the calculation and the experimental differential cross sections[53,54] at T_p = 1 GeV, and correct values of the cross sections at T_p = 1.3 and 1.5 GeV. However, the angular distributions at T_p = 1.3 and 1.5 GeV are poorly accounted for. It is important that at T_p = 1 GeV the main contribution to the scattering is made by one or two resonances but, when the energy increases, the influence of a large number of resonances becomes manifest, and this naturally complicates the analysis.

In this respect, scattering at $T_p < 1$ GeV is much easier to interpret. Indeed, it is shown in ref. 62 that at $T_p \approx$ 400–700 MeV the decisive contribution to the cross section can be made by one resonance $\Delta(3/2, 3/2)$. An advantage of this paper is that it established with the aid of a triangular diagram (see Fig. 31d) a connection between the backward pd scattering and the well investigated process (7) ($pp \to d\pi^+$), by making it possible to avoid the uncertainties that are inevitable in calculations of the type carried out in refs. 63 and 66. The process (7), as is well known, has a resonance character due to excitation of a $\Delta(3/2, 3/2)$ isobar. This circumstance, according to ref. 62, can become manifest in a characteristic nonmonotonicity of the energy behavior of the backward pd scattering. A more accurate calculation[67] did not change the principal predictions of ref. 62. An experiment[16] performed in Dubna revealed no "dip" in the energy dependence of the backward pd-scattering cross section, but has shown that a well pronounced "shoulder" is observed in this dependence (Fig. 32). A similar result was obtained in detailed measurements of the differential cross sections of backward pd scattering, performed by Alder et al.[68] at energies 316–590 MeV. Against the background of the general picture of a rapid decrease of the cross sections with increasing energy (see Fig. 30), this behavior has indeed an anomalous character. Since the diagram of simple nucleon exchange cannot account for this singularity and underestimates by one order of magnitude the cross sections at energies close to 600 MeV, it is natural to relate the observed anomaly with the Craigie–Wilkin "resonance" mechanism.[62]

Thus, at the present time there are grounds for assuming that a correct allowance for the nucleon-exchange diagram and for a process proceeding via excitation of a (3/2, 3/2) isobar suffices for the description of backward pd scattering in the wide energy interval 100–700 MeV.

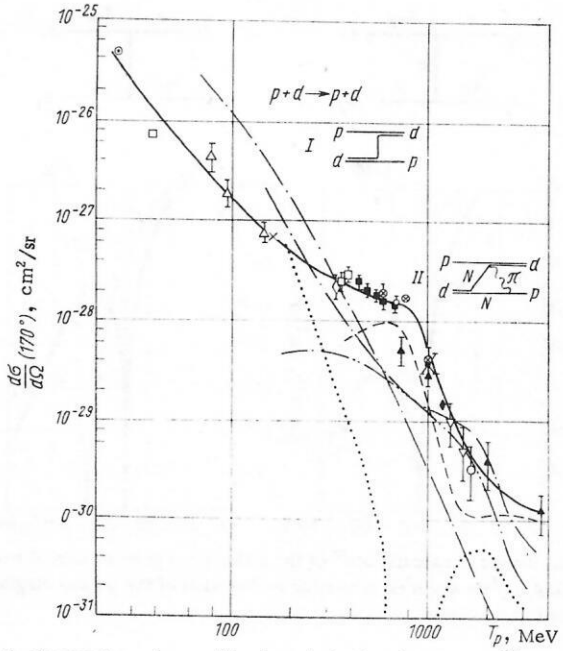

Fig. 32. Energy dependence of backward elastic pd scattering:[15] solid curve – drawn through the point for the sake of clarity. For a bibliography of the experimental papers see ref. 15; dashed curve – results of calculation[62] in accordance with diagram II; the curves calculated from the neutron-pickup diagram (I) with the wave functions of the deuteron are the following: dash–dot curve, – Hulthén function for the S state; dotted and dash–double-dot curve – S and D wave functions of refs. 63 and 64, respectively; double-dash–dot curve – joint contribution of the S and D states with the wave functions of refs. 63 and 64.

An exact separation of the contribution of the individual scattering mechanism calls, of course, for additional measurements. Calculations[69] have shown, in particular, that polarization effects are highly sensitive to the reaction mechanism. Thus, the one-pion scattering model requires absence of quadrupolarization of the recoil deuterons in backward pd scattering and in reaction (7). In addition, the polarization parameter should reverse sign at 1.5 GeV in this model at large scattering angles. Reliable identification of the scattering mechanism will make it possible to obtain, from pd-scattering experiments at $T_p \leq 1$ GeV, direct information on the Fourier components of the deuteron wave function up to ~ 3 F^{-1}.

To interpret the backward scattering of fast protons by the more complicated nuclei ^{3}He and ^{4}He, a "heavy-pickup" mechanism (Fig. 33) was recently proposed.[70] Using the wave function of ^{4}He in the form assumed in ref. 71 for the description of electron scattering, the authors of ref. 70 have obtained agreement between the calculated values of the differential backward-scattering cross section and the data at 150 and 665 MeV. It is typical that the results of the calculation at energies above 200 MeV are very sensitive to the behavior of the wave function at short distances. Thus, if the wave function of the type

$$|\Psi_{^4\mathrm{He}}(r_i)|^2 = N\prod_{i=1}^{4}\exp(-\alpha^2 r_i^2)\left[1 - D\exp\left(-\frac{\alpha^2}{\gamma^2}r_i^2\right)\right], \quad (41)$$

where α^2 = 0.597 F^{-2}, γ^2 = 0.308, and D = 0.858, is replaced by a simple Gaussian function, then the scattering cross section at 670 MeV decreases by several orders of mag-

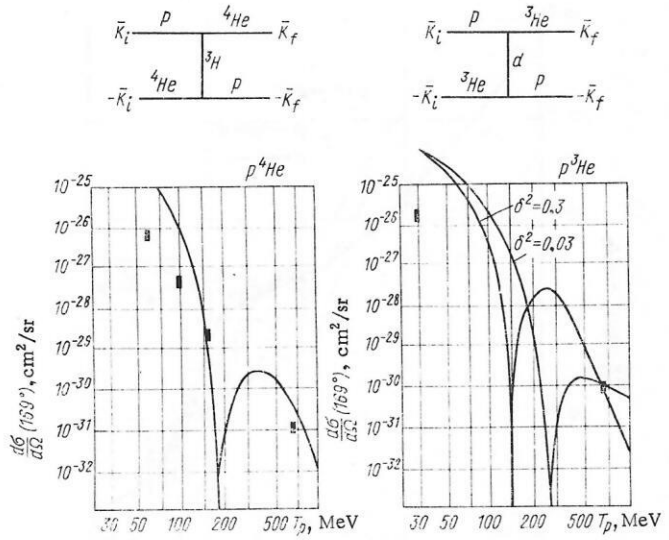

Fig. 33. Results of calculations[70] of the differential cross section of backward elastic p^4He and p^3He scattering on the basis of the pickup diagrams indicated in the figure.

nitude. In the calculation of scattering from ^3He, the wave function was chosen in a form analogous to (41):

$$|\Psi_{^3He}(r_i)|^2 = N' \prod_{i=1}^{3} \exp(-3\beta^2 r_i^2)\left[1 - C\exp\left(-\frac{\beta^2}{\delta^2} r_i^2\right)\right]. \quad (42)$$

In view of the fact that at the time of the calculation there were no experimental data on e^3He scattering at high momentum transfer, the value of δ in (42) was determined by comparing the calculation with the experimental cross section of p^3He scattering at 665 MeV. For C = 1, two values were obtained in ref. 71: $\delta^2 = 0.3$ and $\delta^2 = 0.03$. Later data on the electromagnetic form factor of ^3He up to 20 F^{-2} (ref. 73) show that the position of the dip in the form factor at $q^2 = 12$ F^{-2} and the behavior of the form factor at large q^2 agree well with the predicted value $\delta^2 = 0.03$ at C = 0.4.

Thus, it is not excluded that the discussed mechanism plays the principal role in backward p^3He and p^4He scattering. However, in analogy with pd scattering, we can expect a contribution of triangular diagrams with a pion in the intermediate state also for the case of scattering by helium. In addition to the obvious need for detailed measurements of the angular and energy dependences in backward scattering, an important role in a firm establishment of the scattering mechanism may be played by polarization experiments, the significance of which to the solution of the problem was demonstrated in ref. 72 with backward p^3He scattering as an example.

CONCLUSION

The investigation of the reaction of quasielastic knock-out of fast fragments by high-energy protons is still in the initial stage. There is no doubt that the construction of high-current proton accelerators in the very near future will serve as an impetus to rapid progress in this field. It is, however, clear now that such investigations can produce an important contribution to the solution of many nuclear-physics problems. These problems differ in degree of generality and significance, arise in different aspects of research on knock-out reactions, and sometimes overlap to some degree. Nonetheless, it is expedient in conclusion to list some of them:

1. An elucidation of the mechanism of knock-out reactions, namely a quantitative determination of the contribution of the pole mechanism, and the separation of that part of the reaction amplitude which can be directly attributed to the interaction of the incident proton with the nucleon clusters.

2. An elucidation of the question of separation of effects connected with the interaction of fast knocked-out nucleons in the final state and effects due to correlations of these nucleons in the ground state of the target nucleus.

3. The solution of a question that is closely related with the first two problems, that of the spatial distribution of the nucleon clustering. It is necessary to ascertain whether knock-out reactions can yield, in spite of their peripheral character, information on the clustering in the s-shells of light nuclei.

4. A check on different model representations of nuclei in clustering (the cluster model, the shell model, the nucleon-cluster model), primarily in research of a spectroscopic character.

5. The assessment of the role of the off-mass-shell effects in quasielastic knock-out reactions.

6. Acquisition of information on the short-range correlations between the nucleons making up the clusters.

The experimental data obtained in the experiments performed to date allows us to plan the necessary more accurate and detailed experiments.

[1] G. E. Brown et al., Proc. of Intern. Conf. on High-Energy Phys. and Nucl. Struct., Tokyo (1967).

[2] T. I. Kopaleishvili, in: Problems of Elementary-Particle and Atomic-Nucleus Physics [in Russian], Vol. 2, Atomizdat, Moscow (1971), p. 439.

[3] V. V. Balashov, Proc. Intern. Conf. on Clustering Phenomena in Nucl., Bochum (1969).

[4] Yu. A. Simonov, Yad. Fiz., 3, 630 (1969) [Sov. J. Nucl. Phys., 3, 461 (1966)]; A. M. Badalyan and Yu. A. Simonov, Yad. Fiz., 3, 1032 (1966) [Sov. J. Nucl. Phys., 3, 755 (1966)]; A. I. Baz' et al., Fiz. El. Chast. Atom. Yad., 3, 275 (1972) [Sov. J. Particles Nucl., 3, 137 (1972)].

[5] A. I. Baz', V. F. Demin, and M. V. Zhukov, Yad. Fiz., 9, 1184 (1969) [Sov. J. Nucl. Phys., 9, 693 (1969)]; A. I. Baz' et al., ZhETF Pis. Red., 12, 151 (1970) [JETP Lett., 12, 105 (1970)]; V. F. Rybachenko and A. A. Sadovoi, Yad. Fiz., 12, 710 (1970) [Sov. J. Nucl. Phys., 12, 384 (1971)].

[6] L. S. Azhgirei et al., Zh. Eksp. Teor. Fiz., 33, 1185 (1957) [Sov. Phys.—JETP, 6, 911 (1958)].

[7] R. J. Sutter et al., Phys. Rev. Lett., 19, 1189 (1967).

[8] J. L. Friedes et al., Nucl. Instr. Meth., 54, 1 (1967).

[9] G. W. Benett et al., Phys. Rev. Lett., 19, 387 (1967).

[10] L. S. Azhgirei et al., Yad. Fiz., 13, 6 (1971) [Sov. J. Nucl. Phys., 13, 3 (1971)].

[11] L. S. Azhgirei et al., Communication JINR R1-6380 (1972).

[12] V. P. Dzhelepov, High Energy Phys. and Nucl. Structure, Proc. of the Third Intern. Conf., New York—London, Plenum Press (1970), pp. 278-87.

[13] V. S. Borisov et al., ZhETF Pis. Red., 9, 667 (1966) [JETP Lett., 9, 413 (1966)].

[14] V. I. Komarov et al., Paper at Fifth Intern. Conf. on High-Energy Physics and Atomic Structure, Uppsala (1973).

[15] V. I. Komarov et al., Paper at Fourth Intern. Conf. on High-Energy Physics and Atomic Structure, Dubna (1971) JINR R1-6343 (1972); Yad. Fiz., 16, 234 (1972) [Sov. J. Nucl. Phys., 16, 129 (1973)].

[16] J. C. Alder et al., Phys. Rev., C6, 18 (1972).

[17] J. C. Alder et al., Phys. Rev., C6, 769 (1972).

[18]A. P. Zhdanov, V. N. Kuz'min, and R. M. Yakovlev, Izv. AN SSSR, Ser. Fiz., 29, 239 (1965); Yad. Fiz., 1, 625 (1965) [Sov. J. Nucl. Phys., 1, 447 (1965)]; V. N. Kuz'min and R. M. Yakovlev, Izv. AN SSSR, Ser. Fiz., 29, 1237 (1965).
[19]V. I. Komarov, G. E. Kosarev, and O. V. Savchenko, JINR Preprint R1-4227 (1968).
[20]V. I. Komarov, G. E. Kosarev, and O. V. Savchenko, JINR Preprint R1-4373 (1969).
[21]V. I. Komarov, G. E. Kosarev, and O. V. Savchenko, Yad. Fiz., 11, 711 (1970) [Sov. J. Nucl. Phys., 11, 399 (1970)]; O. V. Savchenko, Z. Tesh, et al., Paper at Fourth Intern. Conf. on High-Energy Physics and Nuclear Structure, Dubna (1971).
[22]V. V. Balashov, A. N. Boyarkina, and I. Rotter, Nucl. Phys., 59, 417 (1965).
[23]P. Beregi et al., Nucl. Phys., 66, 513 (1965).
[24]Yu. K. Akimov, O. V. Savchenko, and L. M. Soroko, Zh. Eksp. Teor. Fiz., 41, 708 (1961) [Sov. Phys.—JETP, 14, 512 (1962)].
[25]V. I. Komarov and O. V. Savchenko, JINR Preprint R1-3720 (1968).
[26]V. I. Komarov, G. E. Kosarev, and O. V. Savchenko, Yad. Fiz., 12, 1229 (1970) [Sov. J. Nucl. Phys., 12, 675 (1971)].
[27]M. G. Meshcheryakov and B. S. Neganov, Dokl. Akad. Nauk SSSR, 100, 677 (1955).
[28]D. I. Blokhintsev, Zh. Eksp. Teor. Fiz., 33, 1295 (1957) [Sov. Phys.—JETP, 6, 995 (1958)].
[29]B. N. Kalinkin and V. L. Shmonin, JINR Communication R4-6298 (1972).
[30]B. N. Kalinkin and V. L. Shmonin, JINR Communication R4-6299 (1972).
[31]V. G. Neudachin and Yu. F. Smirnov, Nuclear Clusters in Light Nuclei [in Russian], Nauka, Moscow (1969).
[32]A. N. Boyarkina, M. A. Yusupov, and V. V. Karapetyan, Preprint (1969).
[33]I. S. Shapiro, Zh. Eksp. Teor. Fiz., 41, 1616 (1961) [Sov. Phys.—JETP, 14, 1148 (1962)]; Nucl. Phys., 28, 244 (1961); Selected Topics in Nuclear Theory, Int. Atomic Energy Agency, Vienna (1963); Usp. Fiz. Nauk, 92, 594 (1967).
[34]I. S. Shapiro and V. M. Kolybasov, Nucl. Phys., 49, 515 (1963).
[35]V. M. Kolybasov and N. Ya. Smorodinskaya, ZhETF Pis. Red., 8, 335 (1968) [JETP Lett., 8, 206 (1968)].
[36]A. Rotsstein and A. Vam Ginneken, Phys. Rev. Lett., 21, 223 (1968).
[37]A. O. Aganyants et al., Phys. Lett., B27, 590 (1968); Nucl. Phys., B11, 79 (1969); Yu. D. Bayukov et al., Phys. Lett., B33, 416 (1970); G. A. Leksin, Paper at Fourth Intern. Conf. of High Energy Physics and Nuclear Structure, Dubna (1971).
[38]V. V. Balashov et al., Zh. Eksp. Teor. Fiz., 37, 1385 (1959) [Sov. Phys.—JETP, 10, 983 (1960)].
[39]V. S. Nadezhdin, N. I. Petrov, and V. I. Satarov, JINR Communication R1-6835 (1972).
[40]V. G. Neudachin, Yu. F. Smirnov, and N. P. Yudin, Zh. Eksp. Teor. Fiz., 37, 1781 (1959) [Sov. Phys.—JETP, 10, 1256 (1960)].
[41]Yu. A. Kudeyarov et al., Nucl. Phys., 65, 529 (1965).
[42]Yu. A. Kudeyarov, Yu. F. Smirnov, and T. A. Chebotarev, Yad. Fiz., 4, 1048 (1966) [Sov. J. Nucl. Phys., 4, 751 (1967)].
[43]Yu. A. Kudeyarov et al., Nucl. Phys., A163, 316 (1971).
[44]A. K. Jain, N. Sarma, and Banerjei, Nucl. Phys., A142, 330 (1970).
[45]D. W. Devins, B. L. Scott, and H. H. Forster, Rev. Mod. Phys., 37, 396 (1965).
[46]D. L. Hendrie et al., UCRL Report, No. 16580 (1960).
[47]C. Ruhla et al., Phys. Lett., 6, 282 (1963).
[48]V. V. Balashov and V. I. Markov, Nucl. Phys., A163, 465 (1971).
[49]A. Poskanzer, G. Butler, and E. Hide, Phys. Rev., C3, 882 (1971).
[50]D. I. Blokhintsev and K. A. Toktarov, JINR Communication R4-4018 (1968).
[51]S. N. Bunker et al., Nucl. Phys., A113, 461 (1968).
[52]Yu. D. Bayukov et al., Yad. Fiz., 3, 283 (1966) [Sov. J. Nucl. Phys., 3, 203 (1966)].
[53]E. Coleman et al., Phys. Rev. Lett., 16, 761 (1966).
[54]G. W. Benett et al., Phys. Rev. Lett., 19, 387 (1967).
[55]V. I. Komarov, G. E. Kosarev, and O. V. Savchenko, JINR Preprint R1-4876 (1969).
[56]C. C. Kim et al., Nucl. Phys., 58, 32 (1964).
[57]W. Selowe and J. M. Teem, Phys. Rev., 112, 1658 (1958).
[58]A. Cormack et al., Phys. Rev., 115, 599 (1958).
[59]T. Y. Li and G. K. Mark, Can. J. Phys., 46, 2645 (1968).
[60]J. N. Chahoud and G. Russo, Nuovo Cimento, 49, 206 (1967).
[61]L. Bertocchi and A. Capella, Nuovo Cimento, 51, 369 (1967).
[62]N. S. Craigie and C. Wilkin, Nucl. Phys., B14, 477 (1969).
[63]A. K. Kerman and L. S. Kisslinger, Phys. Rev., 180, 1483 (1969).
[64]C. N. Bressel et al., Nucl. Phys., A124, 624 (1969).
[65]S. Igo et al., Nucl. Phys., A195, 33 (1972).
[66]J. S. Sharma, V. S. Bhasin, and A. N. Mitra, Nucl. Phys., B35, 466 (1971).
[67]V. M. Kolybasov and N. Ya. Smorodinskaja, Phys. Lett., B37, 272 (1972).
[68]J. C. Alder et al., NASA TMX-6743 (1972).
[69]B. Z. Kopeliovich, Dissertation (1972).
[70]B. Z. Kopeliovich and I. K. Potashnikova, Yad. Fiz., 13, 1032 (1971) [Sov. J. Nucl. Phys., 13, 592 (1971)].
[71]R. Bassel and C. Wilkin, Phys. Rev., 174, 1179 (1968).
[72]B. Z. Kopeliovich and I. K. Potashnikova, JINR Communication R2-6711 (1972).
[73]J. S. McCarthy et al., Phys. Rev. Lett., 25, 884 (1970).